INFORMATION TO USERS

This material was produced from a microfilm copy of the original document. While the most advanced technological means to photograph and reproduce this document have been used, the quality is heavily dependent upon the quality of the original submitted.

The following explanation of techniques is provided to help you understand markings or patterns which may appear on this reproduction.

1. The sign or "target" for pages apparently lacking from the document photographed is "Missing Page(s)". If it was possible to obtain the missing page(s) or section, they are spliced into the film along with adjacent pages. This may have necessitated cutting thru an image and duplicating adjacent pages to insure you complete continuity.

2. When an image on the film is obliterated with a large round black mark, it is an indication that the photographer suspected that the copy may have moved during exposure and thus cause a blurred image. You will find a good image of the page in the adjacent frame.

3. When a map, drawing or chart, etc., was part of the material being photographed the photographer followed a definite method in "sectioning" the material. It is customary to begin photoing at the upper left hand corner of a large sheet and to continue photoing from left to right in equal sections with a small overlap. If necessary, sectioning is continued again — beginning below the first row and continuing on until complete.

4. The majority of users indicate that the textual content is of greatest value, however, a somewhat higher quality reproduction could be made from "photographs" if essential to the understanding of the dissertation. Silver prints of "photographs" may be ordered at additional charge by writing the Order Department, giving the catalog number, title, author and specific pages you wish reproduced.

5. PLEASE NOTE: Some pages may have indistinct print. Filmed as received.

University Microfilms International
300 North Zeeb Road
Ann Arbor, Michigan 48106 USA
St. John's Road, Tyler's Green
High Wycombe, Bucks, England HP10 8HR

77-7954

KENNEY, Donald James, 1947-
STIMULATED BRILLOUIN SCATTERING
IN MAGNETIZED PLASMAS.

The University of Michigan, Ph.D., 1976
Physics, fluid and plasma

Xerox University Microfilms, Ann Arbor, Michigan 48106

STIMULATED BRILLOUIN SCATTERING IN MAGNETIZED PLASMAS

by
Donald James Kenney

A dissertation submitted in partial fulfillment
of the requirements for the degree of
Doctor of Philosophy
(Aerospace Engineering)
in The University of Michigan
1976

Doctoral Committee:

Professor Rudi S.B. Ong, Chairman
Assistant Professor James F. Driscoll
Professor James J. Duderstadt
Professor Terry Kammash
Professor Martin Sichel

DEDICATION

I would like to dedicate this thesis to my father, James E. Kenney, who worked longer and harder for me to reach this goal than I would have ever considered. My success is more attributable to his desire than to my skill.

ACKNOWLEDGMENTS

The author is deeply grateful to Professor Rudi Ong for his support and guidance, not only while working on this thesis, but through my graduate career. This research was sponsored by the Air Force Office of Scientific Research under Grant AFOSR 76-2904.

TABLE OF CONTENTS

	Page
DEDICATION	ii
ACKNOWLEDGMENTS	iii
LIST OF TABLES	v
LIST OF FIGURES	vi
LIST OF APPENDICES	vii
LIST OF SYMBOLS	viii
I. INTRODUCTION	1
II. MAGNETIZED SBS DISPERSION RELATION	11
III. SOLUTION OF DISPERSION RELATION	25
IV. EFFECTS OF BOUNDEDNESS AND INHOMOGENEITIES	44
V. APPLICATION TO EXPERIMENT	51
VI. CONCLUSIONS	70
APPENDIX	72
REFERENCES	92

LIST OF TABLES

Table		Page
1	Plasma Modes, $\phi_\ell = 0$.	26
2	Plasma Modes, ϕ_ℓ Arbitrary.	27
3	Plasma Modes, $\phi_\ell = \pi/2$.	28
4	e-foldings in Helium Z-Pinch.	68
5	e-foldings in Lithium Z-Pinch.	69

LIST OF FIGURES

Figure		Page
1	Parametric Instabilities in Plasmas.	2
2	Z-Pinch.	8
3	Laser-Plasma Facility.	10
4	Scattering Geometry.	21
5	Instability Regimes.	42
6	Field-Free Threshold, Helium.	55
7	Magnetized Threshold, Helium.	56
8	Field-Free Threshold, Lithium.	57
9	Magnetized Threshold, Lithium.	58
10	Magnetized Threshold vs Angle, Helium.	59
11	Magnetized Threshold vs Angle, Lithium.	60
12	Field-Free Growth Rate, Helium.	61
13	Magnetized Growth Rate, Helium.	62
14	Field-Free Growth Rate, Lithium.	63
15	Magnetized Growth Rate, Lithium.	64
16	Radial Density Profile.	65
17	Radial Temperature Profile.	66
18	Radial Magnetic Field Profile.	67

LIST OF APPENDICES

		Page
APPENDIX A:	Electron and Ion Conductivity.	72
APPENDIX B:	Formal Treatment of Dispersion Relation.	76
APPENDIX C:	Linear Damping Rates.	82

LIST OF SYMBOLS

Abbreviations

EM	electromagnetic
ES	electrostatic
SBS	stimulated Brillouin scattering

Roman

a_1, a_2	wave amplitudes
$\underline{B}$	magnetic field vector
$\underline{B}_o$	DC magnetic field
$\underline{B}_\ell$	magnetic field of low frequency wave
$\underline{B}_\pm$	magnetic field of high frequency waves
c	speed of light
c_a	Alfvén speed $(B_o/\sqrt{4\pi\, n_o m_i})$
c_s	ion acoustic speed $(\sqrt{T_e/m_i})$
D	determinant of $\underline{\underline{K}}$
D_e, D_i	electron and ion conductivity determinants
$D_\pm^\ell$	high frequency dispersion relation, longitudinal $\dfrac{\omega_\pm^2}{c^2} - \dfrac{\omega_{pe}^2}{c^2} - \dfrac{3v_{Te}^2 k_\pm^2}{c^2}$
$D_\pm^t$	high frequency dispersion relation, transverse $\dfrac{\omega_\pm^2}{c^2} - \dfrac{\omega_{pe}^2}{c^2} - k_\pm^2$
d_e, d_i	electron and ion dispersion constants

e	electric charge
$\underline{E}$	electric field vector
$\underline{E}_o$	electric field of pump wave
$\underline{E}_o{}^{\ell}{}_{\pm}$	pump electric field in longitudinal $\underline{k}_{\pm}$ reference frame $\underline{E}_o{}^{\ell}{}_{\pm} = \dfrac{(\underline{k}_{\pm} \cdot \underline{E}_o)\,\underline{k}_{\pm}}{\lvert \underline{k}_{\pm} \rvert^2}$
$\underline{E}_o{}^{t}{}_{\pm}$	pump electric field in transverse $\underline{k}_{\pm}$ reference frame $\underline{E}_o{}^{t}{}_{\pm} = \dfrac{\underline{k}_{\pm} \times \underline{E}_o}{\lvert \underline{k}_{\pm} \rvert}$
$\underline{E}_{\ell}$	electric field of low frequency wave
$\underline{E}_{\pm}$	electric field of high frequency waves
$\underline{E}_{NL}$	nonlinear electric field of force $\underline{F}_{NL}$
$\underline{F}_{NL}$	nonlinear ponderomotive force
g	parameter $[\gamma_i T_i/(\gamma_e T_e + \gamma_i T_i)]$
I_o	pump intensity $(cE_o^2/4\pi)$
I_{thresh}	threshold pump intensity
$\underline{j}$	current density
$\underline{J}$	current density
$\underline{J}_{NL}{}^{\pm}$	nonlinear part of current density
K	coupling coefficient $(\lambda' \mu' \sin^2\psi\, E_o^2 c^2)$
$\underline{\underline{K}}$	plasma dielectric tensor
$\underline{\underline{K}}^T$	transpose of $\underline{\underline{K}}$
$\underline{k}$	wave vector
$\underline{k}_{\ell}$	low frequency wave vector

LIST OF SYMBOLS (continued)

$\underline{k}_{+-}$	high frequency wave vector
$\underline{k}_o$	pump wave vector
k'	wave vector mismatch
k_B	Boltzmann constant
L_B	magnetic field scale length
L_N	density scale length
L_T	temperature scale length
m_e	electron mass
m_i	ion mass
n_e	electron number density
n_i	ion number density
n_ℓ	density perturbation of low frequency wave
n_o	equilibrium number density
Q	parameter $\{1 + [(k^2c^2)/\omega_{pe}^2]\}$
$\underline{\underline{Q}}$	tensor of cofactors of $\underline{\underline{K}}^T$
p_e	electron pressure
$\underline{\underline{P}}_r$	radiation pressure tensor
$\underline{r}$	space coordinate
T_e	electron temperature
T_i	ion temperature
t	time
V_1, V_2	wave group velocities
V_ℓ	group velocity of low frequency wave
V_-	group velocity of backscattered wave
$\underline{v}$	velocity

$\underline{v}_e$	electron velocity
$\underline{v}_i$	ion velocity
v_{Te}	electron thermal velocity
x	space direction
x_ℓ	plasma length
$\underline{x}_o$	amplitude of electron oscillation in pump electric field
x_1	parameter $[(\Gamma_2/V_2)(1/\lvert k'(o)\rvert)]$
x_2	parameter $[(\gamma_o/\lvert k'(o)\rvert\lvert V_1V_2\rvert^{1/2})]$
Z	ion charge number
Z_o^2	pump amplitude

Greek

β	ratio of plasma kinetic pressure to magnetic pressure $[(n_o k_B T_e)/(B_o^2/8\pi)]$
γ_c	parameter $[(\Gamma_2/2)(\lvert V_1/V_2\rvert)^{1/2}]$
γ_e	electron ratio of specific heats
γ_i	ion ratio of specific heats
γ_o	homogeneous growth rate
γ_T	parameter $(\Gamma_1\Gamma_2)^{1/2}$
η	parameter
θ	angle between $\underline{k}_o$ and $\underline{k}_\ell$
Γ_1, Γ_2	linear damping rates
Γ_ℓ	low frequency wave damping rate
Γ_-	backscattered wave damping rate

LIST OF SYMBOLS (continued)

λ, λ'	parameter
λ_{De}	electron Debye length
μ, μ'	parameters
ν_{ei}	electron-ion collision frequency
ϕ_ℓ	angle between $\underline{B}_o$ and $\underline{k}_\ell$
ϕ_o	angle between $\underline{B}_o$ and $\underline{k}_o$
ϕ_-	angle between $\underline{B}_o$ and $\underline{k}_-$
σ	plasma conductivity
$\underline{\underline{\sigma}}_e$	electron conductivity tensor
$\underline{\underline{\sigma}}_i$	ion conductivity tensor
ψ	angle between $\underline{E}_o$ and $\underline{k}_-$
ω	wave frequency
ω_{ce}	electron cyclotron frequency $(eB_o/m_i c)$
ω_{ci}	ion cyclotron frequency $(eB_o/m_i c)$
ω_i	imaginary part of frequency ω
ω_{ia}	ion acoustic frequency
ω_ℓ	frequency of low frequency wave
$\omega_{\ell h}$	lower hybrid frequency $(\omega_{ce}\omega_{ci})^{1/2}$
ω_r	real part of frequency ω
ω_o	frequency of pump wave
ω_{pe}	electron plasma frequency $\sqrt{\frac{4\pi n_e e^2}{m_e}}$

ω_{pi}	ion plasma frequency $\sqrt{\frac{4\pi\, n_i e^2}{m_i}}$
ω_1, ω_2	wave frequency
$\omega_{\pm}$	frequencies of high frequency wave

Subscripts

e	electron
i	ion
ℓ	low frequency
NL	nonlinear
o	pump or equilibrium
+	upshifted
-	downshifted

Superscripts

ℓ	longitudinal
$\ell_{\pm}$	longitudinal $\underline{k}_{\pm}$ reference frame
t	transverse
$t_{\pm}$	transverse $\underline{k}_{\pm}$ reference frame

I. INTRODUCTION

1.1 STIMULATED BRILLOUIN SCATTERING

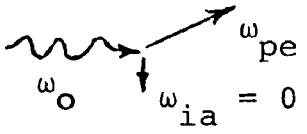
This thesis investigates stimulated Brillouin scattering (SBS) in magnetized plasmas. SBS is one of a class of instabilities known as parametric instabilities (see Fig. 1) and can be characterized by the conversion of an electromagnetic (EM) pump wave into a downshifted EM wave and a low frequency electrostatic (ES) wave. This instability is called parametric because the oscillations of the two excited waves are amplified due to a periodic modulation of a parameter that characterizes the oscillation[21]. The downshifted EM wave is amplified by modulation of plasma currents; the ES wave by modulation of the plasma density.

A mechanism for instability occurs because variations in the currents of the plasma arise directly from density modulations. Coupling of the pump's electric field, $\underline{E}_o$, with background density fluctuations (noise), n_ℓ, produces a perturbation current, $\underline{J}_{NL}^{+}$, which drives another EM wave. The electric field, $\underline{E}_-$, of this second EM wave in turn can beat with the original field, $\underline{E}_o$, to produce a nonlinear force, $\underline{F}_{NL}$, called the ponderomotive force[15]. The plasma fluctuations n_ℓ are enhanced by this low frequency force and, as a result, become the density perturbation associated with a natural ES oscillation in the plasma. Thus a positive feedback mechanism is established by which both $\underline{E}_-$ and n_ℓ grow, resulting in instability.

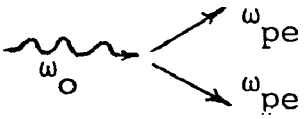
1) ELECTROSTATIC INSTABILITIES



decay instability

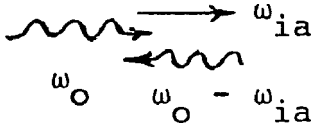


oscillating two stream instability

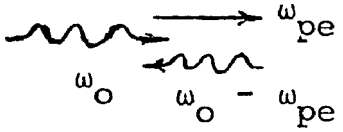


two plasmon decay

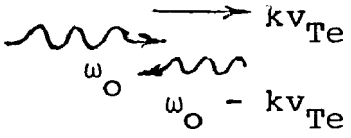
2) ELECTROMAGNETIC INSTABILITIES



stimulated Brillouin scattering (SBS) (see also Fig. 4)



stimulated Raman scattering



stimulated Compton scattering

Figure 1. Parametric Instabilities in Plasmas.
(∿∿∿→ represents EM wave,
⟶ represents ES wave)

Parametric instabilities may be characterized by two properties[21]: 1) a matching condition — the exicted oscillations should satisfy a phase matching condition; 2) a threshold — amplification occurs only when the modulation amplitude exceeds a critical value. For the pump wave, the downshifted wave, and the low frequency wave respectively the wave frequencies can be written as ω_o, ω_- and ω_ℓ and the wave vectors as $\underline{k}_o$, $\underline{k}_-$ and $\underline{k}_\ell$. The phase matching conditions are

$$\omega_o = \omega_- + \omega_\ell \tag{1.1}$$

$$\underline{k}_o = \underline{k}_- + \underline{k}_\ell \tag{1.2}$$

Physically these conditions express conservation of energy and momentum among the interacting waves; mathematically they allow nonlinear terms in the basic equations to be treated as linear in normal mode analysis. The frequency and wave number for each wave must, in addition, satisfy the linear dispersion relation for the plasma, $\omega = \omega(k)$. The dispersion relation then plays an important role in determining which nonlinear resonances are possible. For SBS this requirement causes $\underline{k}_-$ to be directed essentially opposite to $\underline{k}_o$ (Ref. 7). The energy associated with the ω_- wave is then radiated backwards out of the plasma. The matching condition (1.1) shows further that the backscattered wave will be observed at a downshifted frequency.

A threshold for excitation of a parametric instability exists because the natural modes in a plasma are damped. This linear damping must be overcome before parameteric amplification can occur. Each of the various parametric instabilities has a different threshold, and in order to decide which instability will occur in a specific case the respective thresholds and growth rates must be compared.

1.2 IMPORTANCE OF SBS IN LASER FUSION

In order to achieve sufficient compression in laser implosion of pellets to fusion densities[3,22], the focused intensity of the laser must be appreciable. Further the energy in the laser beam must be absorbed in the pellet's plasma corona to drive the shock that causes compression. Classical absorption processes, such as inverse Bremsstrahlung and resonance absorption, are too ineffective to achieve the required energy deposition. However, nonlinear absorption processes may occur for laser power fluxes in excess of 10^{11} watts/cm^2 (Ref. 3).

In particular, the nonlinear parametric instabilities can play an important role in laser-plasma interactions. Some of the parametric instabilities (decay instability, two plasmon decay and oscillating two stream instability) lead to absorption by heating electrons and ions. Other parametric instabilities (stimulated Brillouin scattering, stimulated Raman scattering and stimulated Compton scattering) prevent absorption because these processes scatter the wave

energy of the laser out of the plasma. Other instabilities (modulation and filamentation) alter the laser's focus.

The absorptive instabilities occur near the critical surface in the plasma; the scattering instabilities occur in the underdense region of the plasma through which the laser light must propagate before reaching the critical layer. These scattering instabilities induce the plasma to act as a partially reflecting, dielectric mirror which can lead to substantial reflection of the incident radiation. Thus the fraction of laser energy which can reach the critical surface for absorption can be reduced significantly. Of the scattering instabilities SBS seems to be the most dominant for inhomogeneous plasmas[3]. Thus a complete understanding of this instability is important.

1.3 MAGNETIC FIELDS IN LASER IMPLOSIONS

Direct backscatter thresholds and growth rates were first calculated by Gorbunov[11] in 1968. All of the scattering instabilities including SBS were thoroughly studied by Drake et al.[7] in 1974. Both treatments are deficient however because they assume the plasma is free of DC magnetic fields. In fact such fields can be important in laboratory plasmas[13].

In about 1971 investigators[29] first noticed that large magnetic fields were being generated in laser produced plasmas, such as imploded pellets. Field strengths on the order of a megagauss have been measured[32] first by means of magnetic probes and later by Faraday rotation[31] (a change in

the angle of the plane of polarization of an EM wave propagating along the magnetic field).

Several suggestions[30,31,37,40] have been made for the source of these strong fields. The earliest explanation[31] proposed that the magnetic fields originated from the thermal energy of the plasma and were due to solenoidal electric fields associated with electron temperature and pressure gradients. The magnetic field might be described by an equation of the form

$$\frac{\partial \underline{B}_o}{\partial t} = \nabla \times (\underline{v} \times \underline{B}_o) + \frac{c^2}{4\pi}\frac{1}{\sigma} \nabla^2 \underline{B}_o - \frac{ck_B}{en_o} \nabla n_e \times \nabla T_e \qquad (1.3)$$

where $\underline{B}_o$ is the generated B-field

$\underline{v}$ is the macroscopic fluid velocity

σ is the plasma conductivity

n_e is the electron density

and T_e is the electron temperature.

Another suggested source[31] for the magnetic field is flow energy of the plasma. This dynamo effect has been assumed to be small but may be important when complicated plasma motions develop. For high laser intensities there is a direct conversion between the laser energy and the magnetic field energy[30,31]. Field generation is due to a solenoidal electric field associated with radiation pressure gradients.

$$\frac{\partial \underline{B}_o}{\partial t} = \nabla \times (\underline{v} \times \underline{B}_o) + \frac{c^2}{4\pi}\frac{1}{\sigma} \nabla^2 \underline{B}_o + \frac{c}{e} \nabla \times \frac{1}{n_e} \nabla \cdot \underline{\underline{P}}_r \qquad (1.4)$$

where $\underline{\underline{P}}_r$ is the radiation pressure tensor. More recently it has been suggested that magnetic fields may be generated due to resonance absorption[38]. The averaged forces on the electons due to resonance driven plasma waves produce magnetic fields perpendicular to the plane of incidence.

Whatever sources may be involved in magnetic field generation, the resulting fields are sufficiently large to modify the modes that can propagate in a plasma[9,35]. As a result magnetic fields can influence the excitation of parametric instabilities. As the variety of natural modes is increased due to the presence of the magnetic field, there are new modes that can couple to the pump wave.

The parameteric excitation of electromagnetic waves in magnetized plasmas has received rather limited attention[12]. The difficulty is due to mathematical complexity rather than an understanding of the physical mechanism. The processes involved are the same as for the field free case. Previous investigations by Yu et al.[27,41] and by Manheimer and Ott[18] have been limited to cold plasmas or to restricted geometry. This thesis attempts to provide a comprehensive treatment of SBS. In addition a correspondence with the canonical theory of Nishikawa[20,21] and with the field free theory of Drake[7] is maintained so that the underlying similarity of these parametric instabilities is evident.

1.4 LASER-PLASMA INTERACTION EXPERIMENT

Currently the Nuclear Engineering Department under Dr. D.R. Bach is experimenting with a Z pinch plasma produced

by electrical discharge in a helium gas[33]. A hydrodynamics code[4] and preliminary diagnostics of this plasma indicate electron densities ranging from 10^{17} to 10^{19} particles per cubic centimeter. The corresponding electron plasma frequencies range from 10^{13} to 10^{14} sec^{-1}. The plasma is irradiated with a CO_2 laser; as a result the critical density is approximately 10^{19} cm^{-3}. The experiment is designed to be conducted in a density range that will prevent the excitation of absorptive parametric instabilities which occur near the critical surface. Thus stimulated Brillouin scattering is expected to be the dominant nonlinear instability. The geometry of the experiment is shown in Fig. 2.

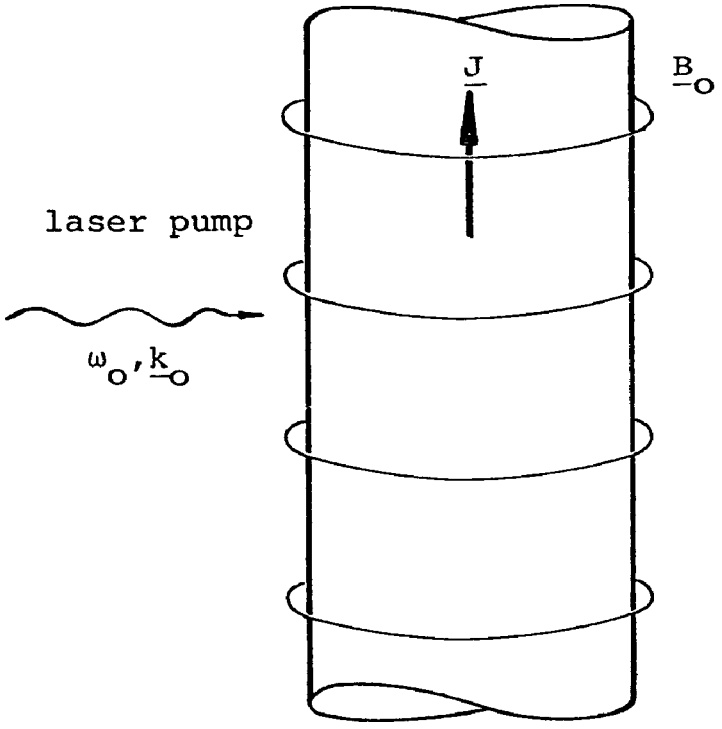


Figure 2. Z-Pinch.

Such a plasma is produced when a metallic wire is exploded or when an electric potential discharges between electrodes in a gaseous atmosphere. The experimental laser-plasma interaction facility is shown in Fig. 3.

There are several reasons why this experiment was chosen. First, the laboratory has experience with the Z-pinch configuration through its use of exploding wires[6]. Second, since the warm, dense plasma is fully developed before the laser pulse, none of the laser energy is lost in preparing the plasma. The laser is only a pump, not a plasma generator. Previous experiments[19,23,39] have used part of the laser pulse to form the test plasma; as a result a detailed accounting of laser energy was impossible. Because of its reproducibility the Z-pinch plasma is an excellent experimental plasma. Further, a well developed hydrodynamics code[4,8] already exists which predicts all the pertinent parameters of the plasma. Finally, since this configuration has the laser beam perpendicular to the magnetic field lines, the effects of the field are most dramatic. This simulates the geometry of imploded pellets.

In summary the problem of stimulated Brillouin scattering in magnetized plasmas has been investigated because 1) megagauss magnetic fields are present in fusion plasmas and SBS may be an important nonlinear phenomena, 2) the theory is appropriate to the experiment at The University of Michigan, and 3) little work has been done for scattering instabilities in magnetized plasmas.

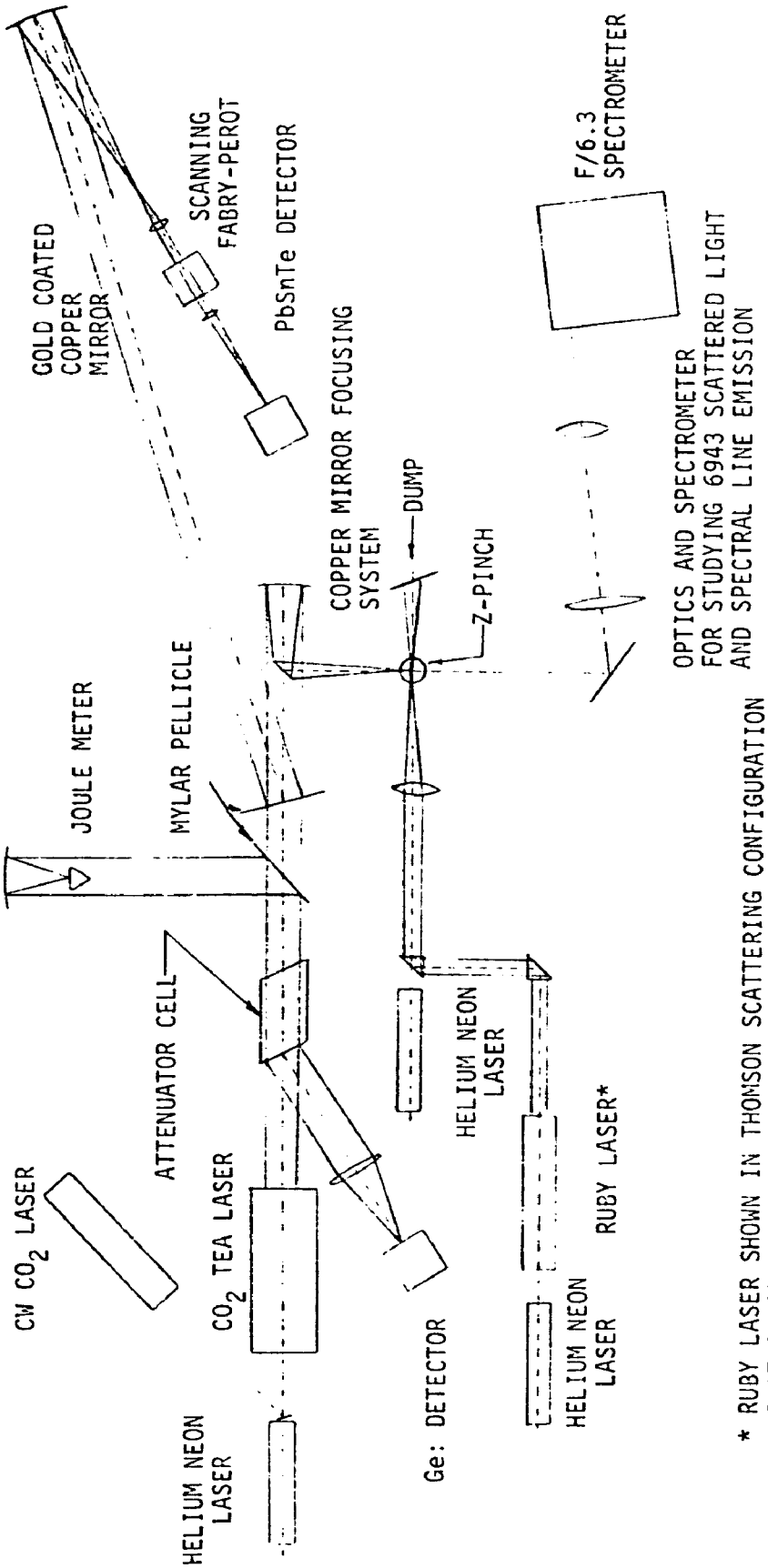


Figure 3. Laser-Plasma Facility.

II. MAGNETIZED STIMULATED BRILLOUIN SCATTERING DISPERSION RELATION

In this chapter the dispersion relation for SBS in magnetized plasmas is developed. First, a general dispersion relation for parametric interactions is derived following the treatment of Manheimer and Ott[18]. Then the dispersion relation, specialized to SBS, is put in the canonical form of the coupled mode oscillator problem of Nishikawa[20,21]. Without further development the equations for threshold and growth rate given by Nishikawa[20] may be used. Several difficulties in the treatment of field free SBS[7] are avoided by this procedure, and the similarity among all parametric processes is emphasized.

2.1 GENERALIZED DISPERSION RELATION

To derive the dispersion relation the strength of the magnetic field is assumed weak so that

$$\omega_o >> \omega_{ce} \quad ;$$

that is the pump frequency, ω_o, is much greater than the electron cyclotron frequency,

$$\omega_{ce} = \frac{eB_o}{m_e c}$$

However, no restriction is imposed on the relative magnitudes of ω_{ce}, ω_{ci} and ω_ℓ where

$$\omega_{ci} = \frac{eB_o}{m_i c}$$

is the ion cyclotron frequency and ω_ℓ is the frequency of the low frequency wave involved in the parametric interaction. Two basic nonlinear effects account for the mode-mode coupling. They are (1) the charged particles feel a low frequency force due to the beating of the high frequency waves which enhances the low frequency mode, and (2) the low frequency wave couples with the pump wave to produce a nonlinear high frequency current which derives the high frequency mode. These two effects lead to the general dispersion relation for parametric instability.

Let the frequency and waves number of the pump be written as $\omega_o, \underline{k}_o$; of the low frequency wave as $\omega_\ell, \underline{k}_\ell$; and of up-shifted and down-shifted high frequency waves as $\omega_{\pm}, \underline{k}_{\pm}$. Conservation of energy and momentum require

$$\omega_{\pm} = \omega_\ell \pm \omega_o \qquad (2.1)$$
$$\underline{k}_{\pm} = \underline{k}_\ell \pm \underline{k}_o$$

The dispersion relation will be obtained by requiring the equation for the low frequency density perturbation, n_ℓ, to have a nontrivial solution. Since the perturbation is caused by the ponderomotive force, $\underline{F}_{NL}$, an expression for it is required. Because the ponderomotive force is due to the beating of the high frequency fields, $\underline{E}_o$ and $\underline{E}_{\pm}$, the high frequency wave equation must be solved. In the derivation that follows first $\underline{E}_{\pm}$ will be obtained, then $\underline{F}_{NL}$, and finally the equation for n_ℓ is derived. Assuming this equation to have a meaningful solution results in the sought dispersion relation.

The high frequency electric field can be written

$$\underline{E} = \underline{E}_o \exp\,[i(\underline{k}_o \cdot \underline{r} - \omega_o t)] + \underline{E}_{\pm} \exp\,[i(\underline{k}_{\pm} \cdot r - \omega_{\pm} t)]$$

$$+ \underline{E}_o^* \exp\,[-i(\underline{k}_o \cdot r - \omega_o t)]$$

$$+ \underline{E}_{\pm}^* \exp\,[-i(\underline{k}_{\pm} \cdot r - \omega_{\pm} t)] \qquad (2.2)$$

where * denotes complex conjugate, $\underline{E}_o$ is the electric field of the pump wave, and $\underline{E}_{\pm}$ is the first order perturbation field of the induced high frequency waves. Assuming that ions do not participate in the high frequency modes, the equations governing $\underline{E}_{\pm}$ are

$$\frac{\partial n_e}{\partial t} + \nabla \cdot (n_e \underline{v}_e) = 0$$

$$\frac{\partial \underline{v}_e}{\partial t} + \underline{v}_e \cdot \nabla\, \underline{v}_e = -\frac{e}{m_e}\left(\underline{E}_{\pm} + \frac{\underline{v}_e \times \underline{B}_o}{c}\right) - 3v_{Te}^2 \frac{\nabla n_e}{n_e}$$

$$\nabla \times \underline{E}_{\pm} = -\frac{1}{c}\frac{\partial \underline{B}_{\pm}}{\partial t}$$

$$\nabla \times \underline{B}_{\pm} = \frac{1}{c}\frac{\partial \underline{E}_{\pm}}{\partial t} + \frac{4\pi}{c}\underline{J}$$

$$\underline{J} = -en_e\underline{v}_e$$

$$\nabla \cdot \underline{E}_{\pm} = -4\pi en_e$$

To solve these equations for $\underline{E}_{\pm}$ the differentials are obtained assuming the variables are of harmonic form, i.e.

$$n_e = n_o + \hat{n}_e \, e^{i(\underline{k}_{\pm} \cdot \underline{r} - \omega_{\pm} t)}$$

Combining the above equations the high frequency wave equation is

$$- \underline{k}_{\pm} \times \underline{k}_{\pm} \times \underline{E}_{\pm} - \frac{\omega_{\pm}^2}{c^2} \underline{E}_{\pm} + \frac{\omega_{pe}^2}{c^2} \underline{E}_{\pm} + \frac{3v_{Te}^2}{c^2} (\underline{k}_{\pm} \cdot \underline{E}_{\pm}) \, \underline{k}_{\pm}$$

$$= i\omega_{\pm} \frac{4\pi}{c^2} \underline{J}_{NL}^{\pm} \qquad (2.3)$$

where $\underline{J}_{NL}^{\pm}$ is the nonlinear part of $\underline{J}$. The current density $\underline{J}$ has linear and nonlinear terms as it is the product of perturbed quantities,

$$\underline{J} = - en_e \underline{v}_e$$

The linear terms of the current density, arising from the product $n_o \hat{\underline{v}}_e$, are the third and fourth terms on the left of Eq. (2.3). The nonlinear current density, $\underline{J}_{NL}^{\pm}$, can be derived from the Vlasov equation[18].

$$\underline{J}_{NL}^{\pm} = \begin{cases} \dfrac{ie^2}{m_e} \dfrac{n_\ell \underline{E}_o}{\omega_+} & \text{for + mode} \\ \dfrac{ie^2}{m_e} \dfrac{n_\ell \underline{E}_o^*}{\omega_-} & \text{for - mode} \end{cases} \qquad (2.4)$$

Making these substitutions for $\underline{J}_{NL}^{\pm}$ Eq. (2.3) becomes

$$- \underline{k}_{\pm} \times \underline{k}_{\pm} \times \underline{E}_{\pm} - \frac{\omega_{\pm}^2}{c^2} \underline{E}_{\pm} + \frac{\omega_{pe}^2}{c^2} \underline{E}_{\pm} + \frac{3v_{Te}^2}{c^2} (\underline{k}_{\pm} \cdot \underline{E}_{\pm}) \, \underline{k}_{\pm}$$

$$= \begin{cases} - \dfrac{\omega_{pe}^2}{c^2} \dfrac{n_\ell}{n_o} \underline{E}_o \\ - \dfrac{\omega_{pe}^2}{c^2} \dfrac{n_\ell}{n_o} \underline{E}_o^* \end{cases} \qquad (2.5)$$

This equation can be easily solved by decomposing it into components in a coordinate system whose axes are longitudinal, ℓ, and transverse, t, with respect to $\underline{k}_+$ and $\underline{k}_-$.

Using the definition

$$\underline{E}_o{}^t = \frac{\underline{k}_+ \times \underline{E}_o}{|\underline{k}_+|} \qquad \underline{E}_o{}^{*t} = \frac{\underline{k}_- \times \underline{E}_o^*}{|\underline{k}_-|}$$
$$\underline{E}_o{}^\ell = \frac{\underline{k}_+ \cdot \underline{E}_o}{|\underline{k}_+|} \frac{\underline{k}_+}{|\underline{k}_+|} \qquad \underline{E}_o{}^{*\ell} = \frac{\underline{k}_- \cdot \underline{E}_o^*}{|\underline{k}_-|} \frac{\underline{k}_-}{|\underline{k}_-|} \tag{2.6}$$

the solution of the wave equation (2.5) is

$$\underline{E}_+{}^t = \frac{\frac{\omega_{pe}{}^2}{c^2} \frac{n_\ell}{n_o} \underline{E}_o{}^t}{D_+{}^t} \qquad \text{with} \qquad D_+{}^t = \frac{\omega_+{}^2}{c^2} - \frac{\omega_{pe}{}^2}{c^2} - k_+{}^2$$

(2.7)

$$\underline{E}_+{}^\ell = \frac{\frac{\omega_{pe}{}^2}{c^2} \frac{n_\ell}{n_o} \underline{E}_o{}^t}{D_+{}^\ell} \qquad \text{with} \qquad D_+{}^\ell = \frac{\omega_+{}^2}{c^2} - \frac{\omega_{pe}{}^2}{c^2} - \frac{3v_{Te}{}^2}{c^2} k_+{}^2$$

The equation for $\underline{E}_-$ are similar except with $\underline{E}_o^*$ instead of $\underline{E}_o$.

Now the quantity n_ℓ must be derived. The force driving the density perturbation n_ℓ is the ponderomotive force[15,26].

$$\underline{F}_{NL} = - \frac{m_e}{2\omega_o{}^2} (e/m_e)^2 \nabla \langle \underline{E} \cdot \underline{E} \rangle \tag{2.8}$$

where $\underline{E}$ is the total high frequency electric field and the brackets indicate an average over the high frequency time scale. The requirements for Eq. (2.8) to be valid are

$$\underline{k}_o \cdot \underline{v} \ll \omega_o \quad , \quad \underline{k}_\ell \cdot \underline{x}_o \ll 1 \quad \text{and} \quad \omega_{ce} \ll \omega_o$$

where $\underline{v}$ is the unperturbed velocity of an individual electron and $\underline{x}_o$ is the amplitude of the oscillation of an electron in the field of the pump wave. The first restriction is satisfied by almost all electrons if

$$v_{Te} \ll c$$

The second restriction requires electron excursions due to the pump to be smaller than the length of the density perturbation of the low frequency wave. No current laser can exceed this condition. The final inequality is the condition for the ponderomotive force to be unaffected by the magnetic field and is satisfied for all cases in this thesis. Since the ponderomotive force varies as the reciprocal of the mass, the force on the ions is much smaller than that on the electrons and will be neglected.

Substituting the expression for the high frequency field, Eq. (2.2), into (2.8) and keeping only those terms which satisfy the matching conditions, Eq. (2.1), the equation for the ponderomotive force becomes

$$\underline{F}_{NL} = - \frac{m_e}{\omega_o^2} \left(\frac{e}{m_e}\right)^2 \nabla \{(\underline{E}_+ \cdot \underline{E}_o^* + \underline{E}_- \cdot \underline{E}_o) \exp [i(\underline{k}_\ell \cdot \underline{r} - \omega_\ell t)] + (\underline{E}_+^* \cdot \underline{E}_o + \underline{E}_-^* \cdot \underline{E}_o^*) \exp [-i(\underline{k}_\ell \cdot \underline{r} - \omega_\ell t)]\} \qquad (2.9)$$

The matching conditions permit the combination of exponential products, such as

$$\exp [i(\underline{k}_+ \cdot \underline{r} - \omega_+ t)] \exp [- i(\underline{k}_o \cdot \underline{r} - \omega_o t)]$$

into simple harmonic terms, as

$$\exp\{i[(\underline{k}_+ - \underline{k}_o)\cdot\underline{r} - (\omega_+ - \omega_o)\,t]\} = \exp[i(\underline{k}_\ell\cdot\underline{r} - \omega_\ell t)]$$

since $\underline{k}_\ell = \underline{k}_+ - \underline{k}_o$ and $\omega_\ell = \omega_+ - \omega_o$. Mathematically then the problem seems linear. Using the solution for $\underline{E}_+$, Eq. (2.7), the ponderomotive force is

$$\underline{F}_{NL} = -\frac{m_e}{\omega_o^2}(e/m_e)^2\,\nabla\left[\frac{\omega_{pe}^2}{c^2}\frac{n_\ell}{n_o}\left(\frac{|E_o{}^{\ell}{}_{+}|^2}{D_+{}^{\ell}} + \frac{|E_o{}^{t}{}_{+}|^2}{D_+{}^{t}} + \frac{|E_o{}^{\ell}{}_{-}|^2}{D_-{}^{\ell}} + \frac{|E_o{}^{t}{}_{-}|^2}{D_-{}^{t}}\right)\right]\exp[\pm i(\underline{k}_\ell\cdot\underline{r} - \omega_\ell t)] \qquad (2.10)$$

where

$$|E_o{}^{t}{}_{\pm}|^2 = \underline{E}_o{}^{t}\cdot\underline{E}_o{}^{*t} = \frac{|\underline{k}_\pm \times \underline{E}_o|^2}{|\underline{k}_\pm|^2}$$

and

$$|E_o{}^{\ell}{}_{\pm}|^2 = \underline{E}_o{}^{\ell}\cdot\underline{E}_o{}^{*\ell} = \frac{|\underline{k}_\pm\cdot\underline{E}_o|^2}{|k_\pm{}^2|}$$

The low frequency response to the ponderomotive force is to be considered. Since the ions are not affected by this force, the equations for $\underline{E}_\ell$, the low frequency perturbation field, can be written

$$\nabla \times \underline{E}_\ell = -\frac{1}{c}\frac{\partial \underline{B}_\ell}{\partial t} \qquad (2.11)$$

$$\nabla \times \underline{B}_\ell = \frac{1}{c}\frac{\partial \underline{E}_\ell}{\partial t} + \frac{4\pi}{c}\,\underline{\underline{\sigma}}_e \cdot (\underline{E}_{NL} + \underline{E}_\ell) + \frac{4\pi}{c}\,\underline{\underline{\sigma}}_i \cdot \underline{E}_\ell \tag{2.12}$$

where $\underline{\underline{\sigma}}_e$ and $\underline{\underline{\sigma}}_i$ are the low frequency electron and ion conductivity tensors. Using harmonic forms for the perturbations these equations can be solved to get

$$\underline{\underline{K}} \cdot \underline{E}_\ell = \frac{4\pi i\omega_\ell}{c^2}\,\underline{\underline{\sigma}}_e \cdot \underline{E}_{NL}$$

or

$$\underline{E}_\ell = \underline{\underline{K}}^{-1} \cdot \frac{4\pi i\omega_\ell}{c^2}\,\underline{\underline{\sigma}}_e \cdot \underline{E}_{NL} \tag{2.13}$$

where

$$\underline{\underline{K}} = -\,\underline{k}_\ell \times \underline{k}_\ell \times \underline{\underline{I}} - \frac{\omega_\ell^2}{c^2}\,\underline{\underline{I}} - \frac{4\pi i\omega_\ell}{c^2}\,\underline{\underline{\sigma}}_e - \frac{4\pi i\omega_\ell}{c^2}\,\underline{\underline{\sigma}}_i \tag{2.14}$$

The solution of Eq. (2.11) and (2.12) for $\underline{E}_\ell + \underline{E}_{NL}$ is

$$\frac{4\pi i\omega_\ell}{c^2}\,\underline{\underline{\sigma}}_e \cdot (\underline{E}_\ell + \underline{E}_{NL}) = -\left[\underline{k}_\ell \times \underline{k}_\ell \times \underline{\underline{I}} + \frac{4\pi i\omega_\ell}{c^2}\,\underline{\underline{\sigma}}_i + \frac{\omega_\ell^2}{c^2}\,\underline{\underline{I}}\right] \cdot \underline{E}_\ell \tag{2.15}$$

Using Eq. (2.13) $\underline{E}_\ell$ can be eliminated on the right of (2.15) to get

$$\underline{E}_\ell + \underline{E}_{NL} = -\,\underline{\underline{K}}^{-1} \cdot \left[\underline{k}_\ell \times \underline{k}_\ell \times \underline{\underline{I}} + \frac{4\pi i\omega_\ell}{c^2}\,\underline{\underline{\sigma}}_i + \frac{\omega_\ell^2}{c^2}\,\underline{\underline{I}}\right] \cdot \underline{E}_{NL} \tag{2.16}$$

The equation for conservation of charge is

$$\frac{\partial}{\partial t}\,(-\,en_\ell) + \nabla \cdot \underline{J} = 0$$

with

$$\underline{J} = \underline{\underline{\sigma}}_e \cdot (\underline{E}_\ell + \underline{E}_{NL})$$

So n_ℓ is

$$n_\ell = \frac{1}{\omega_\ell \epsilon} \underline{k}_\ell \cdot \underline{\underline{\sigma}}_e \cdot \underline{\underline{K}}^{-1} \left[\underline{k}_\ell \times \underline{k}_\ell \times \underline{\underline{I}} + \frac{\omega_\ell^2}{c^2} \underline{\underline{I}} + \frac{4\pi i \omega_\ell}{c^2} \underline{\underline{\sigma}}_i \right] \cdot \underline{E}_{NL} \quad (2.17)$$

With $\underline{E}_{NL}$ given by Eq. (2.10), Eq. (2.17) then is

$$n_\ell = \frac{1}{\omega_\ell \epsilon} \underline{k}_\ell \cdot \underline{\underline{\sigma}}_e \cdot \underline{\underline{K}}^{-1} \cdot i\underline{k}_\ell \cdot \left(\frac{\omega_\ell^2}{c^2} \underline{\underline{I}} + \frac{4\pi i \underline{\underline{\sigma}}_i}{c^2} \right) \frac{e}{m_e} \frac{1}{\omega_o} \frac{\omega_{pe}^2}{c^2} \frac{n_\ell}{n_o}$$

$$\times \left(\frac{|E_{o_+}^{\,t}|^2}{D_+^{\,t}} + \frac{|E_{o_+}^{\,\ell}|^2}{D_-^{\,\ell}} + \frac{|E_{o_-}^{\,t}|^2}{D_-^{\,t}} + \frac{|E_{o_-}^{\,\ell}|^2}{D_-^{\,\ell}} \right)$$

n_ℓ appears both on the right side and left side. The non-trivial solution is

$$D = \frac{\underline{k}_\ell}{\omega_\ell} \cdot \underline{\underline{\sigma}}_e \cdot \underline{\underline{Q}} \cdot i\underline{k}_\ell \cdot \left(\frac{\omega_\ell^2}{c^2} \underline{\underline{I}} + \frac{4\pi i \underline{\underline{\sigma}}_i}{c^2} \right) \frac{\omega_{pe}^2}{m_e \omega_o^2 n_o c^2}$$

$$\times \left(\frac{|E_{o_+}^{\,t}|^2}{D_+^{\,t}} + \frac{|E_{o_+}^{\,\ell}|^2}{D_+^{\,\ell}} + \frac{|E_{o_-}^{\,t}|^2}{D_-^{\,t}} + \frac{|E_{o_-}^{\,\ell}|^2}{D_-^{\,\ell}} \right) \quad (2.18)$$

where $\underline{\underline{K}}^{-1} = \underline{\underline{Q}}/D$, $\underline{\underline{Q}}$ is the cofactor tensor of the transpose of $\underline{\underline{K}}$ and $D = \det \underline{\underline{K}}$. This is the nonlinear dispersion relation of Manheimer and Ott which governs the interaction between a pump wave at ω_o and waves at $\omega_\pm$ and ω_ℓ. Unlike Manheimer and Ott, however, $\underline{\underline{\sigma}}_i$, the ion conductivity tensor, has been left in tensor form so that the assumption $\omega_\ell >> \omega_{ci}$ has not

been made. In all other respects the above derivation follows their treatment[18].

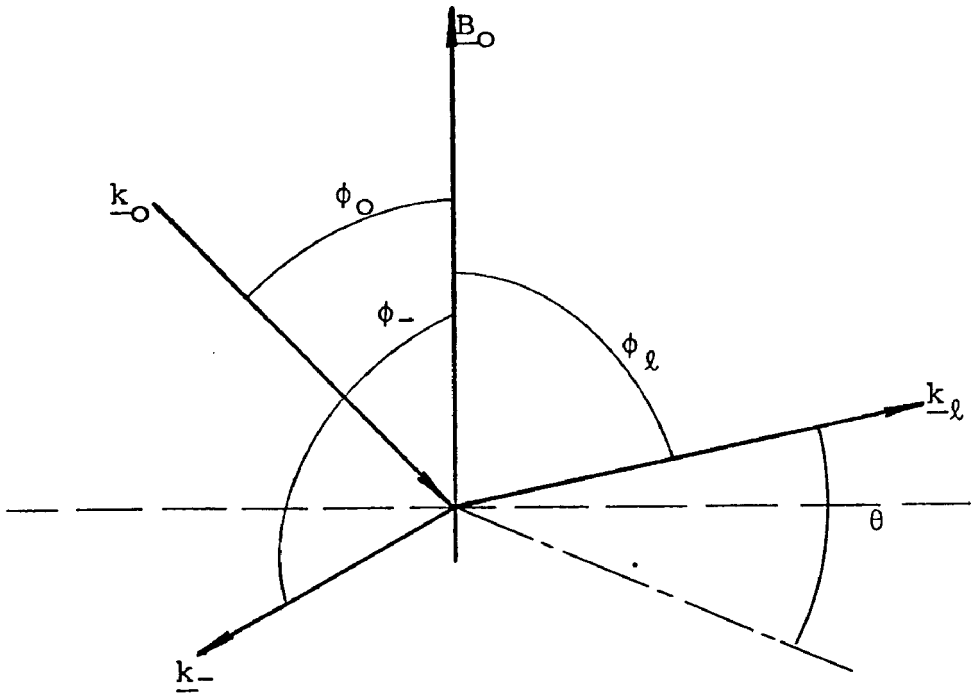
2.2 SBS DISPERSION RELATION

Nishikawa[20] gives the dispersion relation for the coupling of two modes due to the action of a pump wave as

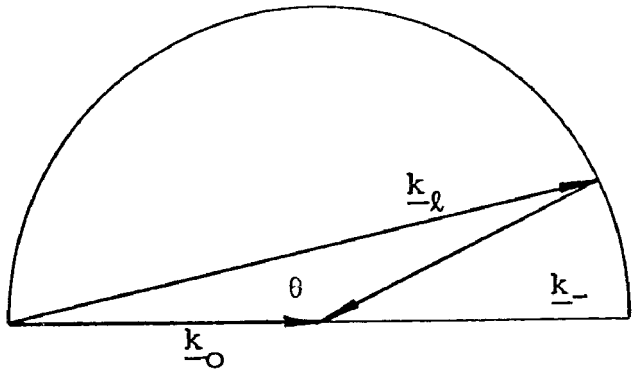
$$(\omega_\ell - \omega_1 + i\Gamma_1)(\omega_\ell - \omega_o + \omega_2 + i\Gamma_2) + \frac{\lambda\mu Z_o^2}{4\omega_1\omega_2} = 0 \qquad (2.19)$$

where ω_1 and ω_2 are the natural frequencies of the two modes, Z_o^2 is the pump power, λ and μ are constants, Γ_1 and Γ_2 are the natural damping rates of the two modes. If the dispersion relation, Eq. (2.18), were put in the form of Eq. (2.19), the equations for threshold and growth rates given by Nishikawa could be used directly. All that would remain is to determine $\lambda\mu Z_o^2$. Furthermore, in this way introduction of damping rates, Γ_ℓ and Γ_-, would be clarified. In the field free treatment of Drake[7] these damping rates are arbitrarily introduced without justification.

First, the general dispersion relation must be particularized to SBS. Since for SBS the downshifted EM mode is amplified, $D_-^t \simeq 0$ is assumed. The remaining terms on the right of Eq. (2.18) are off-resonant and ignored. It is this resonance assumption that restricts the following treatment to SBS. The scattering process is shown diagramatically in Fig. 4a. Because $D_-^t \simeq 0$ and $\underline{k}_- = \underline{k}_\ell - \underline{k}_o$,



4a



4b

Figure 4. Scattering Geometry.

$$k_\ell \simeq 2k_o \cos\theta \tag{2.20}$$

as shown by Drake[7]. The addition of the wave vectors is shown shown in Fig. 4b. From Eq. (2.6)

$$|E_o^{t-}|^2 = |k_- \times \underline{E}_o|^2 / |\underline{k}_-|^2 = \sin^2\psi\, E_o^2 \tag{2.21}$$

where ψ is the angle between $\underline{k}_-$ and $\underline{E}_o$. In general ψ will depend on the state of polarization of the pump wave as well as the angle between $\underline{k}_o$ and $\underline{k}_-$.

In Chapter III [Eqs. (3.11),(3.13), and (3.15)]

$$D = \det \underline{\underline{K}}$$

will be simplified to the form

$$D = \frac{1}{\lambda'}(\omega_\ell^2 - \omega_1^2)$$

where λ' is a constant, and ω_1 is a natural low frequency plasma mode. Since $\omega_\ell \simeq \omega_1$, differing primarily in its imaginary part, D may be approximated

$$D \simeq 2\frac{1}{\lambda'}\omega_1(\omega_\ell - \omega_1) \tag{2.22}$$

By Eq. (2.7)

$$D_-^t = \frac{\omega_-^2}{c^2} - \underline{k}_-\cdot\underline{k}_- - \frac{\omega_{pe}^2}{c^2}$$

But $\omega_- = \omega_\ell - \omega_o$ by Eq. (2.1). So

$$D_-^t = \frac{(\omega_\ell - \omega_o)^2}{c^2} - k_-^2 - \frac{\omega_{pe}^2}{c^2}$$

$$= (\omega_\ell - \omega_o)^2 - \frac{\omega_2^2}{c^2}$$

Since $\omega_\ell - \omega_o \simeq \omega_2$, D_-^t may be approximated

$$D_-^t \simeq \frac{2\omega_2}{c^2}(\omega_\ell - \omega_o - \omega_2) \tag{2.23}$$

Defining

$$\mu' = \frac{\underline{k}_\ell}{\omega_\ell} \cdot \underline{\underline{\sigma}}_e \cdot \underline{\underline{Q}} \cdot i\underline{k}_\ell \cdot \left(\frac{\omega_\ell^2}{c^2} \underline{\underline{I}} + \frac{4\pi i \omega_\ell}{c^2} \underline{\underline{\sigma}}_i \right) \frac{\omega_{pe}^2}{m_e \omega_o^2 n_o c^2} \tag{2.24}$$

the dispersion relation (2.18), using Eqs. (2.21) to (2.24), is then

$$\frac{2}{\lambda'} \omega_1 (\omega_\ell - \omega_1) = \frac{\mu' \sin^2\psi \, E_o^2}{\frac{2\omega_2}{c^2}(\omega_\ell - \omega_o - \omega_2)}$$

or

$$(\omega_\ell - \omega_1)(\omega_\ell - \omega_o - \omega_2) - \frac{\lambda'\mu' \sin^2\psi \, E_o^2 c^2}{4\omega_1\omega_2} = 0 \tag{2.25}$$

With the introduction of natural damping rates, Γ_ℓ and Γ_-, this equation is identical to Eq. (2.19). Note that ω_2 is negative for SBS because of the way the matching condition, Eq. (2.1), was written. Defining the coupling coefficient K as

$$K = \lambda'\mu' \sin^2\psi \, E_o^2 c^2$$

the dispersion relation is

$$(\omega_\ell - \omega_1 + i\Gamma_\ell)(\omega_\ell - \omega_o + |\omega_2| + i\Gamma_-) + \frac{K}{4\omega_1 |\omega_2|} = 0$$

The solution of the dispersion relation gives both the real and imaginary parts of ω_ℓ. Normally one is interested in the real part which is much larger than the imaginary part. In this problem the real frequency is assumed very close to the natural frequency ω_1, thus known. So

$$\omega_\ell \simeq \omega_1 + i\gamma$$

As a result it is the imaginary part that is of interest. Making the above substitution into the dispersion relation results in an expression for the growth rate. As in Nishikawa[20]

$$\gamma = \frac{1}{2}\left\{-(\Gamma_\ell + \Gamma_-) + \left[(\Gamma_\ell - \Gamma_-)^2 + \frac{K}{\omega_1|\omega_2|}\right]^{1/2}\right\} \qquad (2.26)$$

The resulting threshold is

$$\frac{cE_{o_{thres}}^2}{4\pi} = \frac{\omega_1|\omega_2|\Gamma_\ell\Gamma_-}{\pi c \sin^2\psi\ \lambda'\mu'} \qquad (2.27)$$

By comparing Eqs. (2.18) and (2.19), the linear damping rates, Γ_ℓ and Γ_-, have been introduced. Since these dispersion relations are formally the same, previously derived equations for threshold and growth rate can be used. All that remains is to obtain the coupling coefficient K; this will be done in Chapter III.

III. SOLUTION OF THE DISPERSION RELATION

In this chapter the coupling coefficient K will be determined for $\underline{k}_\ell$ propagating at various angles ϕ_ℓ to the uniform magnetic field $\underline{B}_o$ (Fig. 4). Thus det $\underline{\underline{K}}$ and $\underline{\underline{Q}}$ must be calculated. The parameter β compares the relative strengths of the kinetic pressure of the plasma and the magnetic pressure.

$$\beta = \frac{n_o k_B T_e}{B_o^2/8\pi}$$

$$= \frac{2c_s^2}{c_a^2}$$

as $c_s^2 = \frac{k_B T_e}{m_i}$ and $c_a^2 = \frac{B_o^2}{4\pi n_o m_i}$. The linear low frequency modes for a magnetized plasma have been investigated by Stringer[35] in the low β limit, and for arbitrary β by Formisano and Kennel[9]. Their results are summarized in Tables 1 to 3. These are the modes expected to be stimulated as the low frequency wave in SBS. Since the low frequency dispersion relation (see Eq. (8) in Appendix C) is cubic in ω_ℓ^2, an explicit formula cannot be written which contains all the modes. Only for certain approximations can a simple form be given. As a result the equations in the tables are approximate.

TABLE 1. PLASMA MODES,

$\phi_\ell = 0$

$\phi_\ell = 0$, i.e. $\underline{k}_\ell \| \underline{B}_o$

for $\omega_\ell^2 \ll \omega_{ci}^2$, 3 roots	$\omega_\ell^2 = k_\ell^2 c_a^2$	Compressional Alfvén
	$\omega_\ell^2 = k_\ell^2 c_a^2$	Shear Alfvén
	$\omega_\ell^2 = k_\ell^2 c_s^2$	Low frequency acoustic
for $\omega_\ell^2 \simeq \omega_{ci}^2$, 3 roots	$\omega_\ell^2 \simeq k_\ell^2 c_a^2$	Compressional Alfvén
	$\omega_\ell^2 \simeq \omega_{ci}^2$	Ion cyclotron
	$\omega_\ell^2 \simeq \omega_{ci}^2$	Ion cyclotron
for $\omega_\ell^2 \gg \omega_{ci}^2$, 2 roots	$\omega_\ell^2 = \dfrac{c_a^4 k_\ell^4}{\omega_{ci}^2}$	High frequency Alfvén or Whistler
	$\omega_\ell^2 = k_\ell^2 c_s^2$	Intermediate frequency acoustic

Note: $c_s^2 = \dfrac{T_e}{m_i}$, $c_a^2 = \dfrac{B_o^2}{4\pi n_i m_i}$

TABLE 2. PLASMA MODES

ϕ_ℓ Arbitrary

ϕ_ℓ arbitrary

for $\omega_\ell^2 \ll \omega_{ci}^2$, 3 roots

$$\begin{cases} \omega_\ell^2 = k_\ell^2 \left(c_a^2 + c_s^2 \sin^2 \phi_\ell\right) \\ \omega_\ell^2 = k_\ell^2 c_a^2 \cos^2 \phi_\ell \\ \omega_\ell^2 = k_\ell^2 c_s^2 \cos^2 \phi_\ell \end{cases}$$

for $\omega_\ell^2 \simeq \omega_{ci}^2$, 3 roots

$$\begin{cases} \omega_\ell^2 \simeq \dfrac{k_\ell^2 c_a^2}{2Q}\left[1 + \cos^2\phi_\ell\left(1 + \dfrac{k_\ell^2 c_a^2}{Q\,\omega_{ci}^2}\right) + \left\{\left[1 + \cos^2\phi_\ell\left(1 + \dfrac{k_\ell^2 c_a^2}{Q\,\omega_{ci}^2}\right)\right]^2 - 4\cos^2\phi_\ell\right\}^{1/2}\right] \\ \omega_\ell^2 = \omega_{ci}^2\left[1 - \dfrac{Q\omega_{ci}^2}{c_a^2 k_\ell^2}\left(1 + \sec^2\phi_\ell\right)\right] \\ \omega_\ell^2 = \omega_{ci}^2 \cos^2\phi_\ell \end{cases}$$

for $\omega_\ell^2 \gg \omega_{ci}^2$, 2 roots

$$\begin{cases} \omega_\ell^2 \simeq \dfrac{k_\ell^2 c_a^2}{Q}\left(\dfrac{k_\ell^2 c_a^2}{Q\,\omega_{ci}^2}\cos^2\phi_\ell + 1\right) \\ \omega_\ell^2 = k_\ell^2 c_s^2 \end{cases}$$

Note: $Q = 1 + (k_\ell^2 c^2/\omega_{pe}^2)$.

TABLE 3. PLASMA MODES

$\phi_\ell = \pi/2$

$\phi_\ell = \pi/2$; i.e. $\underline{k}_\ell \perp \underline{B}_o$

for $\omega_\ell^2 \ll \omega_{ci}^2$ 1 root	$\omega_\ell^2 = k_\ell^2 (c_a^2 + c_s^2)$	Compressional Alfven
for $\omega_\ell^2 \simeq \omega_{ci}^2$ 1 root	$\omega_\ell^2 = k_\ell^2 \frac{(c_a^2 + c_s^2)}{\Omega}$	Compressional Alfven - high frequency Alfven transition
for $\omega_\ell^2 \gg \omega_{ci}^2$ 1 root	$\omega_\ell^2 = k_\ell^2 \frac{(c_a^2 + \Omega c_s^2)}{\Omega}$	High frequency Alfven

Now the coupling coefficient K will be obtained. The dispersion relation to be solved was derived in Chapter II as

$$D = \frac{\underline{k}_\ell}{\omega_\ell} \cdot \underline{\underline{\sigma}}_e \cdot \underline{\underline{Q}} \cdot i\, \underline{k}_\ell \cdot \left(\frac{\omega_\ell^2}{c^2} \underline{\underline{I}} + \frac{4\pi i \omega_\ell}{c^2} \underline{\underline{\sigma}}_i \right) \frac{\omega_{pe}^2}{m_e \omega_o^2 n_o c^2} \frac{E_o^2 \sin^2\psi}{D_-^t} \tag{3.1}$$

where

$$\underline{\underline{K}} = - \underline{k}_\ell \times \underline{k}_\ell \times \underline{\underline{I}} - \frac{\omega_\ell^2}{c^2} \underline{\underline{I}} - \frac{4\pi i \omega_\ell}{c^2} (\underline{\underline{\sigma}}_e + \underline{\underline{\sigma}}_i)$$

$\underline{\underline{Q}}$ - matrix of cofactors of $\underline{\underline{K}}^T$

$$D_-^t = \frac{(\omega_\ell - \omega_o)^2}{c^2} - (\underline{k}_\ell - \underline{k}_o) \cdot (\underline{k}_\ell - \underline{k}_o) - \frac{\omega_{pe}^2}{c^2}$$

$\underline{\underline{\sigma}}_e, \underline{\underline{\sigma}}_i$ - the electron and ion conductivity tensors are derived in Appendix A.

Four basic assumptions are made to treat the terms in Eq. (3.1).

1) $T_i \simeq 0$, the ions are considered cold

2) $\frac{\omega_\ell^2}{k_\ell^2} << T_e/m_e$, the phase velocity is less than the electron thermal velocity

3) $\frac{\omega_\ell^2}{k_\ell^2} << c^2$, we are dealing with the low frequency, slow waves

4) $\omega_\ell^2 << \omega_{pi}^2 << \omega_{pe}^2$

No assumption is made concerning the size of the parameter β. However only the case $\omega_\ell^2 >> \omega_{ci}^2$ will be considered. In

Chapter V it will be shown that this is the case appropriate of The University of Michigan experiment. Using these assumptions, the elements of the electron conductivity tensor are

$$\sigma_{e_{11}} = \frac{i\omega_{pe}^2}{4\pi\omega_\ell} \frac{1}{d_e} \left(k_\ell^2 \frac{T_e}{m_e} + \omega_{ce}^2 \sin^2 \phi_\ell \right)$$

$$\sigma_{e_{12}} = -\sigma_{e_{21}} = \frac{\omega_{pe}^2}{4\pi\omega_\ell^2} \frac{1}{d_e} k_\ell^2 \frac{T_e}{m_e} \cos \phi_\ell$$

$$\sigma_{e_{13}} = \sigma_{e_{31}} = \frac{i\omega_{pe}^2}{4\pi\omega_\ell} \frac{1}{d_e} \omega_{ce}^2 \sin \phi_\ell \cos \phi_\ell$$

$$\sigma_{e_{22}} = \frac{i\omega_{pe}^2}{4\pi\omega_\ell} \frac{1}{d_e} k_\ell^2 \frac{T_e}{m_e}$$

$$\sigma_{e_{23}} = -\sigma_{e_{32}} = -\frac{\omega_{pe}^2}{4\pi} \frac{1}{d_e} \omega_{ce} \sin \phi_\ell$$

$$\sigma_{e_{33}} = -\frac{i\omega_{pe}^2}{4\pi} \frac{1}{d_e} (\omega_{ce}^2 \cos^2 \phi_\ell - \omega_\ell^2) \qquad (3.2)$$

with

$$d_e = \omega_{ce}^2 + k_\ell^2 \frac{T_e}{m_e} \left(1 - \frac{\omega_{ce}^2}{\omega_\ell^2} \right) \cos^2 \phi_\ell$$

The elements of the ion conductivity tensor are

$$\sigma_{i_{11}} = \sigma_{i_{22}} = \sigma_{i_{33}} = -\frac{i\omega_{pi}^2}{4\pi} \frac{\omega_\ell}{d_i}$$

$$\sigma_{i_{12}} = -\sigma_{i_{21}} = \frac{\omega_{pi}^2}{4\pi} \frac{\omega_{ci}}{d_i} \cos \phi_\ell$$

$$\sigma_{i_{13}} = \sigma_{i_{31}} = \frac{i\omega_{pi}^2}{4\pi\omega_\ell^2} \frac{1}{d_i} \omega_{ci}^2 \cos \phi_\ell \sin \phi_\ell$$

$$\sigma_{i_{23}} = -\sigma_{i_{32}} = \frac{\omega_{pi}^2}{4\pi} \frac{\omega_{ci}}{d_i} \sin \phi_\ell \qquad (3.3)$$

with $$d_i = - \omega_\ell^2$$

Here the coordinate system has been chosen so that $\underline{k}_\ell$ is in the $\underline{Z}$-direction and $\underline{B}_o$ is in the X-Z plane.

The elements of the tensor $\underline{\underline{K}}$ can now be formed after dropping small terms as

$$K_{11} = k_\ell^2 + \frac{\omega_{pe}^2}{c^2} \frac{k_\ell^2 (T_e/m_e)}{\omega_{ce}^2} \frac{1}{\eta} + \frac{\omega_{pe}^2}{c^2} \frac{\sin^2 \phi_\ell}{\eta} \tag{3.4}$$

$$K_{12} = - K_{21} = \frac{i\omega_{pi}^2}{c^2 \omega_{ci}} \frac{\cos \phi_\ell}{\omega_\ell} \left(\omega_{ci}^2 - k_\ell^2 \frac{T_e}{m_e} \frac{1}{\eta} \right) \tag{3.5}$$

$$K_{13} = K_{31} = \frac{\cos \phi_\ell \sin \phi_\ell}{c^2} \left(\frac{\omega_{pe}^2}{\eta} - \omega_{pi}^2 \frac{\omega_{ci}^2}{\omega_\ell^2} \right) \tag{3.6}$$

$$K_{22} = k_\ell^2 + \frac{\omega_{pe}^2}{c^2} \frac{k_\ell^2 (T_e/m_e)}{\omega_{ce}^2} \frac{1}{\eta} \tag{3.7}$$

$$K_{23} = - K_{32} = \frac{i\omega_{pi}^2}{c^2 \omega_{ci}} \frac{\sin \phi_\ell}{\omega_\ell} \left(\omega_{ci}^2 + \frac{\omega_\ell^2}{\eta} \right) \tag{3.8}$$

$$K_{33} = \frac{\omega_{pe}^2}{c^2} \frac{\cos^2 \phi_\ell}{\eta} - \frac{\omega_{pe}^2}{c^2} \frac{\omega_\ell^2}{\omega_{ce}^2} \frac{1}{\eta} + \frac{\omega_{pi}^2}{c^2} \tag{3.9}$$

where

$$\eta = 1 + \frac{k_\ell^2 (T_e/m_e)}{\omega_{ce}^2} - \cos^2 \phi_\ell \frac{k_\ell^2 (T_e/m_e)}{\omega_\ell^2} \tag{3.10}$$

These equations are difficult to handle without making assumptions concerning the order of magnitude of the various terms. To allow ordering the terms the equations will be solved for three ranges of the angle ϕ_ℓ: $\phi_\ell \simeq 0, \pi/4, \pi/2$.

First for $\phi_\ell \simeq 0, \cos\phi_\ell \simeq 1$ and $\sin\phi_\ell \simeq 0$. So sine terms can be neglected.

$$\eta \simeq -\cos^2\phi_\ell \frac{k^2 (T_e/m_e)}{\omega_\ell^2}$$

$$K_{11} = K_{22}$$

and K_{13}, K_{31}, K_{23}, and K_{23} are small because they are sine terms. With similar simplification to the other terms of $\underline{\underline{K}}$

$$D = \det \underline{\underline{K}} = K_{33}\,(K_{11}K_{22} + K_{12}^2)$$

$$= -\frac{\omega_{pi}^2}{c^2 k_\ell^2 c_s^2}\,(\omega_\ell^2 - k_\ell^2 c_s^2)\left(k_\ell^4 - \frac{\omega_{pi}^4}{c^4\omega_{ci}^4}\frac{\omega_\ell^2}{\cos^2\phi_\ell}\right)$$

$$= \frac{\omega_{pi}^2}{c^2}\frac{\omega_{ci}^2}{k_\ell^2 c_s^2 c_a^4}\,(\omega_\ell^2 - k_\ell^2 c_s^2)\left(\omega_\ell^2 - k_\ell^4\frac{c_a^4\cos^2\phi_\ell}{\omega_{ci}^2}\right)$$

The natural modes (see Table 1) are the ion acoustic and whistler waves. Now

$$\underline{\underline{Q}} = \begin{bmatrix} K_{11}K_{33} & -K_{12}K_{33} & 0 \\ K_{12}K_{33} & K_{11}K_{33} & 0 \\ 0 & 0 & K_{11}^2 + K_{12}^2 \end{bmatrix}$$

and

$$\sigma_{e_{31}} = \sigma_{e_{32}} = \sigma_{i_{31}} = \sigma_{i_{32}} = 0$$

So the term in the dispersion relation (3.1)

$$\frac{\underline{k}_\ell}{\omega_\ell}\cdot\underline{\underline{\sigma}}_e\cdot\underline{\underline{Q}}\cdot i\underline{k}_\ell\cdot\left(\frac{\omega_\ell^2}{c^2}\,\underline{\underline{I}} + \frac{4\pi i\omega_\ell}{c^2}\,\underline{\underline{\sigma}}_i\right)$$

becomes simply (see Eq. (5) in Appendix B)

$$-\frac{4\pi\, k_\ell^2}{c^2}\,\sigma_{e_{33}}\,Q_{33}\,\sigma_{i_{33}}$$

Making the necessary substitutions this becomes

$$\frac{k_\ell^2\omega_{pi}^4}{4\pi c^2 k_\ell^2 c_s^2}\,\frac{\omega_{ci}^2}{c_a^4}\left(\omega_\ell^2 - k_\ell^4\,\frac{c_a^4}{\omega_{ci}^2}\cos^2\phi_\ell\right)$$

The whistler wave appears on both sides of the dispersion relation and cancels. The coupling coefficient K is

$$K = \lambda'\mu'\,\sin^2\psi\,E_o^2c^2$$

Here

$$D = \frac{1}{\lambda'}\,(\omega_\ell^2 - k^2c_s^2) \tag{3.11}$$

with

$$\frac{1}{\lambda'} = \frac{\omega_{pi}^2}{c^2}\,\frac{1}{k_\ell^2c_s^2}\,\frac{\omega_{ci}^2}{c_a^4}\left(\omega_\ell^2 - k_\ell^2\,\frac{c_a^4\cos^2\phi_\ell}{\omega_{ci}^2}\right)$$

and

$$\mu' = \frac{k_\ell^2\omega_{pi}^2}{4\pi c^2k_\ell^2c_s^2}\,\frac{\omega_{ci}^2}{c_a^4}\left(\omega_\ell^2 - k_\ell^2\,\frac{c_a^4\cos^2\phi_\ell}{\omega_{ci}^2}\right)\frac{\omega_{pe}^2}{m_en_o\omega_o^2c^2}$$

so

$$K = k_\ell^2 \frac{\omega_{pi}^2}{\omega_o^2} \frac{e^2}{m_e^2} \sin^2\psi \; E_o^2 \tag{3.12}$$

Now for $\phi_\ell \simeq \pi/4$, $\sin \phi_\ell \simeq \cos \phi_\ell$ and

$$\eta \simeq - \cos^2 \phi_\ell \frac{k_\ell^2 (T_e/m_e)}{\omega_\ell^2}$$

Simplifying the terms of $\underline{\underline{K}}$ it is found

$$K_{13}^2 >> K_{23}^2$$

and

$$K_{12}K_{33} >> K_{13}K_{23}$$

so

$$D = K_{11}^2 K_{33} - K_{11}K_{13}^2 + K_{12}K_{33}$$

$$= \frac{\omega_{pi}^2}{c^2} \frac{k_\ell^4}{k_\ell^2 c_s^2} (\omega_\ell^2 - k_\ell^2 c_s^2) - \frac{\omega_{pi}^4}{c^4} \frac{k_\ell^2 \omega_\ell^4}{k_\ell^4 c_s^4} \frac{\sin^2 \phi_\ell}{\cos^2 \phi_\ell}$$

$$+ \frac{\omega_{pi}^6}{c^6 \omega_{ci}^2} \frac{\omega_\ell^2}{\cos^2 \phi_\ell} \frac{(\omega_\ell^2 - k_\ell^2 c_s^2)}{k_\ell^2 c_s^2}$$

$$\simeq \frac{\omega_{pi}^2}{c^2} \frac{(\omega_\ell^2 - k_\ell^2 c_s^2)}{k_\ell^2 c_s^2} \frac{\omega_{ci}^2}{c_a^4 \cos^2 \phi_\ell}$$

$$\times \left(\omega_\ell^2 - \frac{k_\ell^4 c_a^4}{\omega_{ci}^2} \cos^2 \phi_\ell \right)$$

These are the same modes found for $\phi_\ell \simeq 0$ and agree with Table 2. The term in the dispersion relation (3.1)

$$\frac{\underline{k}_\ell}{\omega_\ell} \cdot \underline{\underline{\sigma}}_e \cdot \underline{\underline{Q}} \cdot i\underline{k}_\ell \cdot \left(\frac{\omega_\ell^2}{c^2} \underline{\underline{I}} + \frac{4\pi i \omega_\ell}{c^2} \underline{\underline{\sigma}}_i \right)$$

expands as [Eq. (B.5)]

$$\begin{aligned} - \frac{4\pi\, k_\ell^2}{c^2} [& \sigma_{e_{31}} (Q_{11}\, \sigma_{i_{31}} + Q_{12}\, \sigma_{i_{32}} + Q_{13}\, \sigma_{i_{33}}) \\ & + \sigma_{e_{32}} (Q_{21}\, \sigma_{i_{31}} + Q_{22}\, \sigma_{i_{32}} + Q_{23}\, \sigma_{i_{33}}) \\ & + \sigma_{e_{33}} (Q_{31}\, \sigma_{i_{31}} + Q_{32}\, \sigma_{i_{32}} + Q_{33}\, \sigma_{i_{33}})] \end{aligned}$$

Each of the nine terms above must be investigated separately as to their respective magnitudes. In this tedious task it is found that the last term $\sigma_{e_{33}}\, Q_{33}\, \sigma_{i_{33}}$ is dominant. This is the same term that was dominant for $\phi_\ell \simeq 0$. In this case the term is

$$- \frac{4\pi k_\ell^2}{c^2} \frac{\omega_{pe}^2}{4\pi(-i\omega_\ell)} \frac{1}{d_e} \frac{\omega_{pi}^2}{4\pi(-i\omega_\ell)} \frac{1}{d_i} \omega_\ell^2 \frac{\omega_{ce}^2 \omega_{ci}^2}{c_a^4}$$

$$\times (\omega_\ell^2 - k_\ell^4 c_a^4 \cos^2 \phi_\ell)$$

which simplifies to

$$\frac{k_\ell^2}{4\pi} \frac{\omega_{pi}^4}{c^2} \frac{\omega_{ci}^2}{c_a^2} \frac{1}{k_\ell^2 c_s^2} \frac{1}{\cos^2 \phi_\ell} \left(\omega_\ell^2 - k_\ell^4 c_a^4 \frac{\cos^2 \phi_\ell}{\omega_{ci}^2} \right)$$

Cancelling like terms gives

$$D = \frac{1}{\lambda'} \left(\omega_\ell^2 - k_\ell^2 c_s^2\right) \tag{3.13}$$

with

$$\frac{1}{\lambda'} = \frac{\omega_{pi}^2}{c^2} \frac{\omega_{ci}^2}{k_\ell^2 c_s^2} \frac{1}{c_a^4} \frac{1}{\cos^2\phi_\ell} \left(\omega_\ell^2 - k_\ell^4 \frac{c_a^4 \cos^2\phi_\ell}{\omega_{ci}^2}\right)$$

and

$$\mu' = \frac{k_\ell^2}{4\pi} \frac{\omega_{pi}^4}{c^2} \frac{\omega_{ci}^2}{k_\ell^2 c_s^2} \frac{1}{c_a^4} \frac{1}{\cos^2\phi_\ell} \left(\omega_\ell^2 - k_\ell^4 \frac{c_a^4 \cos^2\phi_\ell}{\omega_{ci}^2}\right) \frac{\omega_{pe}^2}{m_e n_o \omega_o^2 c^2}$$

so

$$K = \lambda'\mu' \sin^2\psi E_o^2 c^2$$

$$= k_\ell^2 \frac{\omega_{pi}^2}{\omega_o^2} \frac{e^2}{m_e^2} \sin^2\psi E_o^2 \tag{3.14}$$

Thus for $\omega_\ell^2 >> \omega_{ci}^2$, $\phi_\ell \simeq \pi/4$, the stimulated low frequency mode is the ion acoustic mode. Note that K is the same as derived previously for $\phi_\ell \simeq 0$.

Now for $\phi_\ell \simeq \pi/2$, $\cos\phi_\ell \simeq 0$ and $\sin\phi_\ell \simeq 1$. So cosine terms can be neglected.

$$\eta \simeq 1 + \frac{k_\ell^2 (T_e/m_e)}{\omega_{ce}^2}$$

and K_{12}, K_{21}, K_{13} and K_{31} are small. With like simplification of the other terms of $\underline{\underline{K}}$

$$D = \det \underline{\underline{K}} = K_{11}(K_{22}K_{33} + K_{23}^2)$$

$$= K_{11}\left[\left(k_\ell^2 + \frac{\omega_{pe}^2}{c^2}\frac{k_\ell^2(T_e/m_e)}{\omega_{ce}^2 + k_\ell^2(T_e/m_e)}\right)\right.$$

$$\times\left(\frac{\omega_{pi}^2}{c^2} - \frac{\omega_{pe}^2}{c^2}\frac{\omega_\ell^2}{\omega_{ce}^2 + k_\ell^2(T_e/m_e)}\right)$$

$$\left. - \frac{\omega_{pe}^4}{c^4}\frac{\omega_{ce}^2\,\omega_\ell^2\sin^2\phi_\ell}{[\omega_{ce}^2 + k_\ell^2(T_e/m_e)]^2}\right]$$

$$= -\frac{\omega_{pe}^6}{c^6}\frac{\left(\frac{k_\ell^2c^2}{\omega_{pe}^2} + \frac{\omega_{ce}^2\sin^2\phi_\ell + k_\ell^2(T_e/m_e)}{\omega_{ce}^2 + k_\ell^2(T_e/m_e)}\right)^2}{[\omega_{ce}^2 + k_\ell^2(T_e/m_e)]}$$

$$\times\left\{\omega_\ell^2 - \frac{k_\ell^2\left[c_a^2 + \left(1 + \frac{k_\ell^2c^2}{\omega_{pe}^2}\right)c_s^2\right]}{\left(\frac{k_\ell^2c^2}{\omega_{pe}^2} + \frac{\omega_{ce}^2\sin^2\phi_\ell + k_\ell^2(T_e/m_e)}{\omega_{ce}^2 + k_\ell^2(T_e/m_e)}\right)}\right\}$$

For $\phi_\ell = \pi/2$, $\sin\phi_\ell = 1$ and this corresponds to the mode given in Table 3 called the high frequency Alfven wave. Note that the approximations involved in this case resulted in a suppression of the ion acoustic mode. Now

$$\underline{\underline{Q}} = \begin{bmatrix} K_{22}K_{33} + K_{23}^2 & 0 & 0 \\ 0 & K_{11}K_{33} & -K_{11}K_{23} \\ 0 & K_{11}K_{23} & K_{11}K_{22} \end{bmatrix}$$

and $\sigma_{i_{31}} = \sigma_{e_{31}} = 0$. So the term in the dispersion relation (3.1)

$$\frac{\underline{k}_\ell}{\omega_\ell} \cdot \underline{\underline{\sigma}}_e \cdot \underline{\underline{Q}} \cdot i\underline{k}_\ell \cdot \left(\frac{\omega_\ell^2}{c^2} \underline{\underline{I}} + \frac{4\pi i \omega_\ell}{c^2} \underline{\underline{\sigma}}_i \right)$$

expands as

$$- \frac{4\pi k_\ell^2}{c^2} \left[\sigma_{e_{32}} \left(K_{11}K_{33}\sigma_{i_{32}} - K_{11}K_{23}\sigma_{i_{33}} \right) + \sigma_{e_{33}} \left(K_{11}K_{23}\sigma_{i_{32}} + K_{11}K_{22}\sigma_{i_{33}} \right) \right]$$

This simplifies to

$$- \frac{4\pi k_\ell^2}{c^2} \frac{\omega_{pe}^2}{4\pi(-i\omega_\ell)} \frac{1}{d_e} \frac{\omega_{pi}^2}{4\pi(-i\omega_\ell)} \frac{1}{d_i} K_{11}$$

$$\times \left\{ \omega_\ell^4 k_\ell^2 + \omega_\ell^4 \frac{\omega_{pe}^2}{c^2} \frac{\omega_{ce}^2 \sin^2 \phi_\ell}{\left[\omega_{ce}^2 + k_\ell^2 (T_e/m_e)\right]} + \omega_\ell^4 \frac{\omega_{pe}^2}{c^2} \frac{k_\ell^2 (T_e/m_e)}{\left[\omega_{ce}^2 + k_\ell^2 (T_e/m_e)\right]} \right\}$$

$$= - \frac{k_\ell^2}{4\pi} \frac{\omega_{pe}^6}{c^6} \frac{\omega_{pi}^2}{\left[\omega_{ce}^2 + k_\ell^2 (T_e/m_e)\right]}$$

$$\times \left(\frac{k_\ell^2 c^2}{\omega_{pe}^2} + \frac{\omega_{ce}^2 \sin^2 \phi_\ell + k_\ell^2 (T_e/m_e)}{\omega_{ce}^2 + k_\ell^2 (T_e/m_e)} \right)^2$$

The coupling coefficient K is

$$K = \lambda' \mu' \sin^2\psi \; E_o^2 c^2$$

Here

$$\omega_1^2 = \frac{k_\ell^2 \left[c_a^2 + \left(1 + \frac{k_\ell^2 c^2}{\omega_{pe}^2} \right) c_s^2 \right]}{\frac{k_\ell^2 c^2}{\omega_{pe}^2} + \frac{[\omega_{ce}^2 \sin^2 \phi_\ell + k_\ell^2 (T_e/m_e)]}{[\omega_{ce}^2 + k_\ell^2 (T_e/m_e)]}} \tag{3.15}$$

and

$$D = \frac{1}{\lambda'} (\omega_\ell^2 - \omega_1^2)$$

with

$$\frac{1}{\lambda'} = - \frac{\omega_{pe}^6}{c^6} \frac{\left(\frac{k_\ell^2 c^2}{\omega_{pc}^2} + \frac{\omega_{ce}^2 \sin^2 \phi_\ell + k_\ell^2 (T_e/m_e)}{\omega_{ce}^2 + k_\ell^2 (T_e/m_e)} \right)^2}{[\omega_{ce}^2 + k_\ell^2 (T_e/m_e)]}$$

and

$$\mu' = - \frac{k_\ell^2}{4\pi} \frac{\omega_{pe}^6}{c^6} \frac{\omega_{pi}^2}{[\omega_{ce}^2 + k_\ell^2 (T_e/m_e)]}$$

$$\times \left(\frac{k_\ell^2 c^2}{\omega_{pe}^2} + \frac{\omega_{ce}^2 \sin^2 \phi_\ell + k_\ell^2 (T_e/m_e)}{\omega_{ce}^2 + k_\ell^2 (T_e/m_e)} \right)^2 \frac{\omega_{pe}^2}{m_e n_o \omega_o^2 c^2}$$

So

$$K = k_\ell^2 \frac{\omega_{pi}^2}{\omega_o^2} \frac{e^2}{m_e^2} \sin^2\psi \; E_o^2 \qquad (3.16)$$

Thus for $\omega_\ell^2 >> \omega_{ci}^2$, $\phi_\ell \simeq \pi/2$, the stimulated low frequency mode is the high frequency Alfvén wave. Note that K is the same as for both of the other cases investigated.

At this point some general remarks can be made about SBS in magnetized plasmas. Comparison with the growth rate given by Drake[7] shows that the coupling coefficient K is the same in both the magnetized and field free cases. Differences appear in ω_ℓ, the frequency of the low frequency stimulated wave which obeys a different dispersion relation, and in Γ_ℓ, the linear damping rate. Allowing the imposed field to go to zero in the work above, recovers the results of Drake.

Previously published results for magnetized SBS can also be compared. Yu et al.[41] calculated growth rates and thresholds for a cold, magnetized plasma ($\beta = 0$) with the restricted geometry $\phi_\ell = \pi/2$ and $\theta = 0$. The low frequency mode is the lower hybrid resonance, $\omega_{\ell h} = (\omega_{ci}\omega_{ce})^{1/2}$. Setting $T_e = 0$ in Eq. (3.15) recovers this result. Shukla et al.[27] and Lee[16] considered the case $\phi_\ell = 0$ and $\theta = 0$. They found field free SBS to be unchanged for stimulation along the magnetic field lines. Equation (3.11) also shows this result. In Appendix B it is shown that irregardless of magnetic field strength (the ratio $\omega_\ell^2/\omega_{ci}^2$ arbitrary) the stimulated Brillouin scattering process remains unchanged from the field-free case for propagation along field lines.

This should be expected. Manheimer and Ott[18] investigated scattering off whistler waves in a cold plasma ($\beta = 0$) with rather inconclusive results. The treatment here shows that temperature effects are important. So to rederive their results the plasma would have to be assumed cold from the beginning of the derivation.

The possibility of a wave being stimulated by SBS is better understood by a consideration of the polarization of the low frequency waves. For $\omega_\ell^2 > \omega_{ci}^2$ the ion acoustic wave is purely electrostatic for those angles at which it propagates. Stringer[35] shows that the propagation region is $\cos^2 \phi_\ell > m_e/m_i$. The high frequency Alfvén wave (whistler wave) is in general a mixed ES-EM or hybrid mode except for $\phi_\ell = \pi/2$. For cross field propagation the wave polarization is electrostatic. $\phi_\ell \simeq \pi/2$ is the range in which the ion acoustic wave does not propagate. The low frequency component of the SBS instability seems preferentially to be an electrostatic mode.

In summary for $\omega_\ell^2 > \omega_{ci}^2$, the ion acoustic wave [Eqs. (3.11) and (3.13)] is stimulated except for $\phi_\ell \simeq \pi/2$. In that case the high frequency Alfvén wave [Eq. (3.15)] is excited.

$$\omega_\ell^2 = \begin{cases} k_\ell^2 c_s^2 & \text{if } \cos^2 \phi_\ell > m_e/m_i \\ & \text{(ion acoustic wave)} \\ k_\ell^2 \left[\dfrac{c_a^2}{\left(1 + \dfrac{k_\ell^2 c^2}{\omega_{pe}^2}\right)} + c_s^2 \right] & \text{if } \cos^2 \phi_\ell < m_e/m_i \\ & \text{(high frequency Alfven wave)} \end{cases} \tag{3.17}$$

The instability regions are illustrated in Fig. 5.

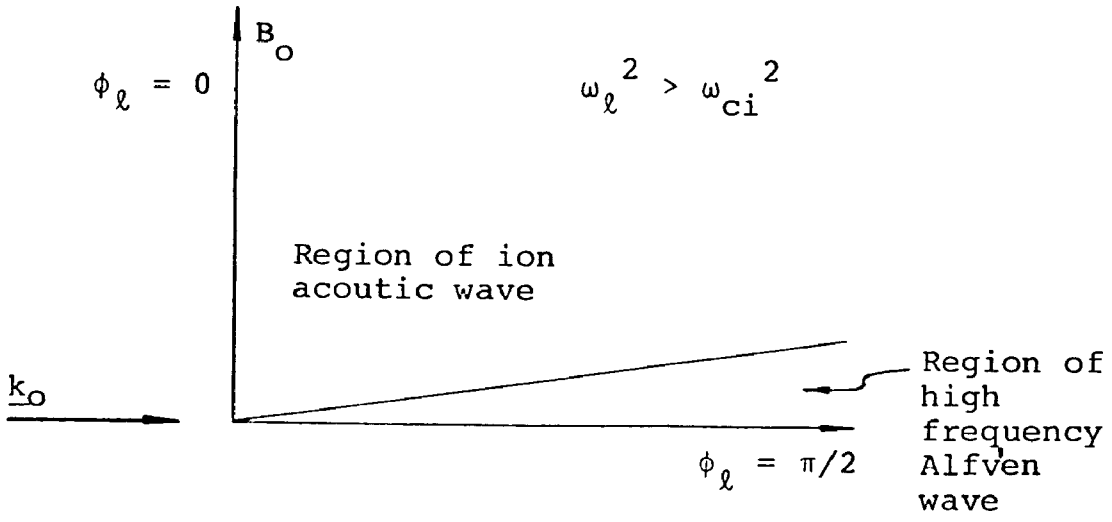


Figure 5. Instability Regimes.

The effect of the magnetic field may be explained as follows: With no magnetic field the beating of the $\underline{E}_o$ and $\underline{E}_-$ wave fields forces the oscillation in n_ℓ to be an ion acoustic wave. In the presence of a magnetic field the plasma particles are not able to move freely across magnetic field lines. Thus the longitudinal ion acoustic wave has difficulty propagating across the magnetic field. However, there are magnetoacoustic waves which can propagate across field lines. For the case $\omega_\ell > \omega_{ci}$ the ion acoustic mode is drastically modified only when $\phi_\ell \simeq \pi/2$. This means the effect of the magnetic field is slight unless $\underline{k}_\ell$ is almost perpendicular to $\underline{B}_o$. When $\phi_\ell = \pi/2$, ω_ℓ becomes the high frequency Alfvén wave. Both the ion acoustic wave and the high frequency Alfvén wave are longitudinal modes for appropriate angles.

From Eqs. (2.26),(2.27),(3.11)-(3.16), the laser threshold intensity for instability and the growth rate of the instability are

$$I_{thresh} = \frac{c}{\pi} \frac{\omega_\ell \omega_- \Gamma_\ell \Gamma_-}{\omega_{pi}^2 \frac{e^2}{m_e^2} \frac{k_\ell^2}{\omega_o^2} \sin^2\psi} \tag{3.18}$$

$$\gamma = \frac{1}{2} \left\{ - (\Gamma_\ell + \Gamma_-) + \left[(\Gamma_\ell - \Gamma_-)^2 + \omega_{pi}^2 \frac{e^2}{m_e^2} \frac{k_\ell^2}{\omega_o^2} \frac{E_o^2 \sin^2\psi}{\omega_\ell \omega_-} \right]^{1/2} \right\} \tag{3.19}$$

IV. EFFECTS OF BOUNDEDNESS AND INHOMOGENITIES

Up to this point the plasma under consideration has been assumed to be infinite and homogeneous. To apply the results to laboratory plasmas, the effects of boundedness and nonuniformities must be considered. Inhomogenities and the finite length of the plasma can stabilize parametric instabilities by limiting the region where the phase matching conditions [Eq. (2.1)] are satisfied exactly. Therefore, the absolute or convective nature[2] of the instability must be known. Convective instabilities are important only if significant growth occurs before the instability saturates due to wave vector mismatch outside the unstable region.

Many researchers[17,24,25] have investigated parametric instabilities in bounded, inhomogeneous plasmas. Since these studies begin with equations for wave amplitudes a_1 and a_2,

$$\frac{\partial a_1}{\partial t} + V_1 \frac{\partial a_1}{\partial x} + \Gamma_1 a_1 = \gamma_o a_2 \exp\left[i\int_0^x k'(x)\, dx\right] \qquad (4.1)$$

$$\frac{\partial a_2}{\partial t} + V_2 \frac{\partial a_2}{\partial x} + \Gamma_2 a_2 = \gamma_o a_1 \exp\left[-i\int_0^x k'(x)\, dx\right] \qquad (4.2)$$

where k' is the wave vector mismatch, γ_o is the homogeneous growth rate, and V_1 and V_2 are wave group velocities, they are independent of any particular parametric process. The results are applied to a specific instability by specifying γ_o, V_1 and V_2, and k'. Pesme, Laval, and Pellat[24] give the

most concise summary of the effects of boundedness and inhomogeneity. Since SBS has been found to be a convective instability, the equations from Pesme, Laval, and Pellat give the number of exponentiations (e-foldings) of the amplified waves above initial noise levels before the instability saturates by convection. Although the growth necessary to observe a backscattered signal will depend on the particular plasma, the minimum number of e-foldings needed for detection is usually assumed to be ten (Ref. 39).

Several new quantities are defined as follows.

x is the size of finite plasma

$$k' = d/dx\ [k_{ox}(x) - k_{1x}(x) - k_{2x}(x)] \qquad (4.3)$$

where the inhomogeneity is in the x-direction; k_{ox}, k_{1x}, k_{2x} are the components of the wave vectors in that direction.

V_1 is the group velocity of wave $\underline{k}_1$

V_2 is the group velocity of wave $\underline{k}_2$

where it is assumed $|V_1| >> |V_2|$

and $|\Gamma_1/V_1| << |\Gamma_2/V_2|$

γ_o is the growth rate of the parametric instability in the homogeneous case

$$\gamma_c = \Gamma_2/2\ |V_1/V_2|^{1/2}$$

$$\gamma_T = (\Gamma_1\Gamma_2)^{1/2}$$

$$x_1 = \Gamma_2/V_2\ (1/|k'(o)|) \quad ; \quad x_2 = \gamma_o/\left(|k'(o)|\,|V_1V_2|^{1/2}\right)$$

The number of e-foldings as given by Pesme can be found in one of the regimes below.

1) If $\gamma_c > \gamma_T > \gamma_o$, there are no e-foldings

2) If $\gamma_c > \gamma_o > \gamma_T$ and

   a) if $x_\ell < x_1$, boundedness is dominant and

   $$[(\gamma_o^2/|V_1|\Gamma_2) - (\Gamma_1/|V_1|)]\, x_\ell \tag{4.4}$$

   gives the number of e-foldings

   b) if $x_1 < x_\ell$, the nonuniformities are dominant and

   $$\pi\gamma_o^2/|V_1V_2k'(o)| \tag{4.5}$$

   gives the number of e-foldings

3) If $\gamma_o >> \gamma_c >> \gamma_T$, linear damping is unimportant and

   a) if $x_2 >> x_\ell$, boundedness is dominant and

   $$\gamma_o x_\ell/|V_1V_2| \tag{4.6}$$

   gives the number of e-foldings

   b) if $x_\ell >> x_2$, the nonuniformities are dominant and

   $$\pi\gamma_o^2/|V_1V_2k'(o)| \tag{4.7}$$

   gives the number of e-foldings.

Since $V_1 >> V_2$ is assumed, for SBS k_1 is the high frequency wave and k_2 is the low frequency wave. To apply the above equations the wave vector mismatch must be obtained, as magnetic inhomogeneities have not been treated in the literature, new equations for the wave vector mismatch will now be derived. Sidescatter as well as backscatter will be considered since the sideways propagating wave moves parallel

to the inhomogeneities and is not affected by it. The side-scatter instability may grow more than the backscatter instability and thus be more important. From Chapter III the equations for backscatter are ($\underline{k}_o \perp \underline{B}_o$ and $\underline{k}_- \perp \underline{B}_o$)

$$k_{ox} = k_o = \frac{[\omega_o^2 - \omega_{pe}^2(x)]^{1/2}}{c}$$

$$k_{1x} = k_- = \frac{[\omega_-^2 - \omega_{pe}^2(x)]^{1/2}}{c}$$

$$k_{2x} = k_\ell = \omega_\ell \left[\frac{c_a^2(x)}{Q(x)} + c_s^2(x)\right]^{1/2}$$

so

$$\frac{dk_{ox}}{dx} = -\frac{1}{2k_o c^2}\frac{d}{dx}[\omega_{pe}^2(x)]$$

$$\frac{dk_{-x}}{dx} = -\frac{1}{2k_- c^2}\frac{d}{dx}[\omega_{pe}^2(x)]$$

$$\frac{dk_{\ell x}}{dx} = -\frac{1}{2}\frac{k_\ell}{(c_a^2/Q + c_s^2)} \times \left\{\frac{Q\frac{d}{dx}[c_a^2(x)] - c_a^2\frac{d}{dx}[Q(x)]}{Q} + \frac{d}{dx}[c_s^2(x)]\right\}.$$

With

$$\frac{d}{dx}\left[\omega_{pe}^{2}(x)\right] = \frac{4\pi e^{2}}{m_e}\frac{d}{dx}\left[n_e(x)\right]$$

$$\frac{d}{dx}\left[c_a^{2}(x)\right] = \frac{1}{4\pi m_i n_i^{2}} \times \left\{2n_i B_o \frac{d}{dx}\left[B_o(x)\right] - B_o^{2}\frac{d}{dx}\left[n_i(x)\right]\right\}$$

$$\frac{d[Q(x)]}{dx} = -\frac{16\pi e^{2}\omega_o^{2}}{m_e\,\omega_{pe}^{4}}\frac{d}{dx}\left[n_e(x)\right]$$

$$\frac{d[c_s^{2}(x)]}{dx} = \frac{1}{m_i}\frac{d}{dx}\left[T_e(x)\right]$$

and scale lengths defined as

$$L_N = \left[\frac{1}{n_e}\left|\frac{dn_e}{dx}\right|\right]^{-1}$$

$$L_T = \left[\frac{1}{T}\left|\frac{dT}{dx}\right|\right]^{-1}$$

$$L_B = \left[\frac{1}{B_o}\left|\frac{dB_o}{dx}\right|\right]^{-1}$$

so that

$$\frac{d[n_e(x)]}{dx} = \frac{n_e}{L_N} \quad ; \quad \frac{d[T_e(x)]}{dx} = \frac{T_e}{L_T} \quad ; \quad \frac{d[B_o(x)]}{dx} = \frac{B_o}{L_B}$$

the equation for mismatch becomes

$$k' = \frac{1}{2} \frac{k_\ell^3}{\omega_\ell} \left(\frac{2c_a^2}{Q} \frac{1}{L_B} + \frac{c_s^2}{L_T} \right) \tag{4.8}$$

The equations for sidescatter are ($\underline{k}_o \perp \underline{B}_o$ and $k_- \| \underline{B}_o$)

$$k_{ox} = k_o = \frac{[\omega_o^2 - \omega_{pe}^2(x)]^{1/2}}{c}$$

$$k_{1x} = 0$$

$$k_{2x} = |\underline{k}_\ell| \cos 45° = \frac{\omega_\ell}{c_s(x)} \cos 45°$$

It can be seen from Fig. 4 that $\theta = 45°$ for sidescatter. So

$$\frac{dk_{ox}}{dx} = - \frac{1}{2k_o c^2} \frac{d[\omega_{pe}^2(x)]}{dx}$$

$$\frac{dk_{1x}}{dx} = 0$$

$$\frac{dk_{2x}}{dx} = - \frac{1}{2} \frac{k_\ell \cos 45°}{c_s^2} \frac{d}{dx} [c_s^2(x)]$$

Using the equations above the mismatch becomes

$$k' = - \frac{\omega_{pe}^2}{2k_o c^2} \frac{1}{L_N} + \frac{k_\ell \cos 45°}{2L_T} \tag{4.9}$$

Equation (4.9) is the same for both field free and magnetized SBS. However, Eq. (4.8) shows that in the magnetized case the additional nonuniformity of the magnetic field causes

the wave vector mismatch to be more severe. Less growth probably will result. The equations needed to calculate growth of the SBS instability for finite, inhomogeneous, magnetized plasmas have been derived. In the next chapter these results will be applied to the laser-plasma interaction experiment at The University of Michigan.

V. APPLICATION TO EXPERIMENT

Large laser fusion facilities currently in use produce focused intensities in excess of 10^{14} watts/cm^2; many small installations achieve intensities above 10^{10} watts/cm^2. The equations developed in the preceding chapters can be used to predict the occurrence and behavior of stimulated Brillouin scattering in such applications. In this chapter graphs are presented which show the threshold and growth rates for irradiated plasmas. The ranges of plasma density and temperature chosen are appropriate to the laser-plasma interaction experiment at The University of Michigan. Calculations are performed for helium and lithium. Plasma densities vary from 10^{17} to 10^{19} cm^{-3}; temperatures from 10 to 30 ev. The electrons and ions are assumed to have equal temperatures. The magnetic field strength is taken to be 30 kilogauss.

A characteristic property of parametric instabilities is the existence of a threshold. The first graphs presented, Figs. 6-9, display the pump wave intensity required for growth of the instability. The pertinent equations are the equations for threshold (3.18), the low frequency dispersion relation (3.17), and the natural damping rates [(C.2) and (C.4)]. To appreciate the effect of the magnetic field, field free calculations have also been performed (Figs. 6 and 8). The results of Chapter III can be used in the limit of vanishing magnetic field provided unmodified Landau damping

is used for the decrement of the low frequency wave. For the magnetized plasmas typically $\omega_\ell = 10^{10}$ sec^{-1} and $\omega_{ci} = 10^8$ sec^{-1} so the assumption $\omega_\ell >> \omega_{ci}$ is valid. Comparison of the graphs shows that the thresholds for the magnetized plasma are lower. This results because the high frequency Alfvén wave is less strongly damped than the ion acoustic wave. Also, for the magnetized case the threshold is weakly dependent on density until near the critical density (10^{19} cm^{-3}). In neither case is temperature dependence very strong. In magnetized plasmas the dispersion relation and the damping rate of the low frequency wave are strongly dependent on the scattering angle θ between the pump wave vector and the low frequency wave vector. A comparison of the thresholds for instability for various angles is shown in Figs. 10 and 11. These plots show that the threshold for direct backscatter ($\theta = 0$) is lowest.

Growth rates can be calculated for both these cases using Eq. (3.19). The field free case for helium and lithium is shown in Figs. 12 and 15; Figs. 14 and 16 present results for magnetized plasmas. The pump intensity is chosen to be 10^{11} watts/cm^2, a number typical for the laser used at The University of Michigan and in many other small facilities (Refs. 19, 23, 39). This intensity is at least an order of magnitude above threshold for the parameter ranges chosen here. Comparison shows that the growth rates for each case are almost identical. This results because at intensities well

above threshold the important parameter in the calculation is the damping rate of the high frequency wave. This number is practically the same for all situations. It should be noted that growth rates for laser intensities close to threshold may be as small as 10^6 sec^{-1}. Since the laser pulse time scale for powerful lasers is on the order of a few nanoseconds, there would not be time for noticeable growth. As a result the practical threshold is somewhat higher.

To further refine the analysis of the laser-plasma interaction experiment of The University of Michigan, effects of boundedness and inhomogeneities must be considered. The equations derived in Chapter IV are applicable for this purpose. The Z-pinch plasmas used in the experiment are produced either by the discharge of an electric potential in helium or by exploding lithium wire. Parameters describing these plasmas are calculated by a one-dimensional hydrodynamics code[4,8] develoepd for this type plasma. The radial variation of density, temperature and magnetic field for helium and lithium are shown in Figs. 16-18. In both cases $\omega_\ell \simeq 10^{10}$ sec^{-1} and $\omega_{ci} \simeq 10^8$ sec^{-1} so the results of Chapter III are valid. Since SBS is a convective instability, wave vector mismatch caused by inhomogeneities will limit growth of the instability. Equations (4.4) to (4.7) of Chapter IV can be used to calculate the number of e-foldings of the amplified waves above noise levels that will occur in each region. Table 4 shows the expected growth for

helium; Table 5 for lithium. For each of ten regions radially into the plasma the tables list the pertinent equation for the calculation and the resulting number of e-foldings. For pump intensity of 10^{11} watts/cm^2 measureable scattering should occur for both plasmas. For the helium plasma growth is so great the instability will saturate by pump depletion. As a result, practically all the laser energy will be scattered out of the plasma.

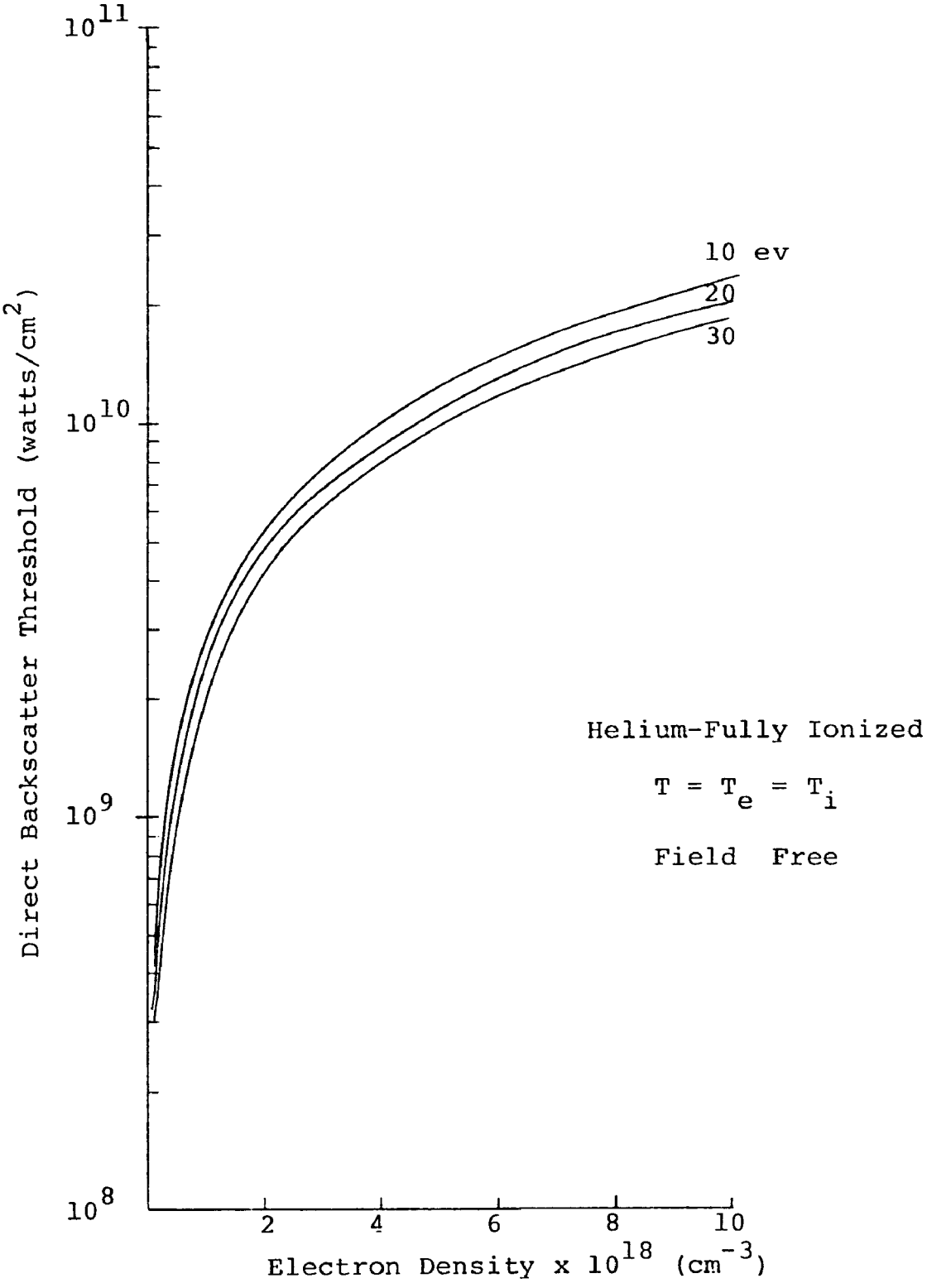


Figure 6. Field-Free Threshold, Helium.

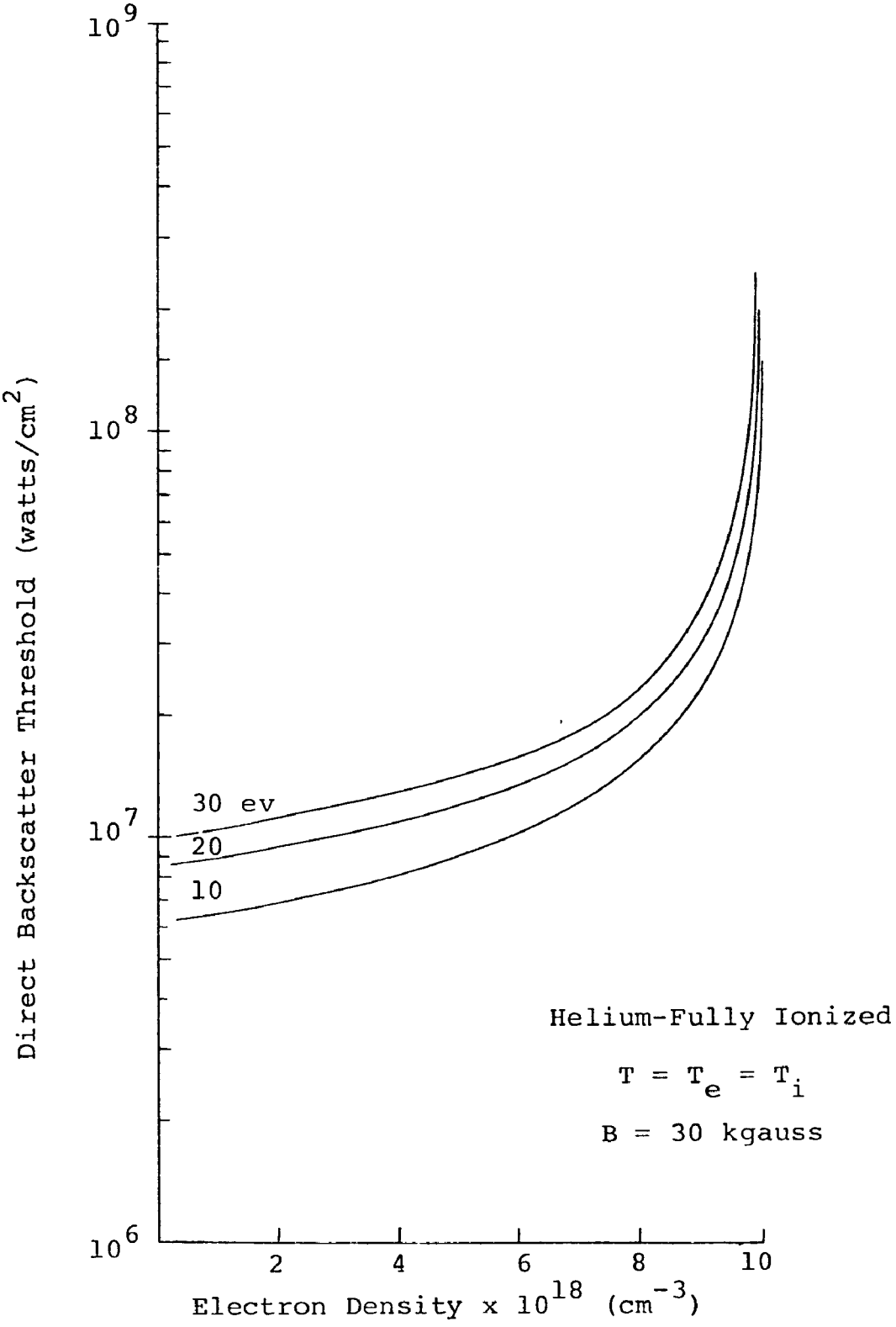


Figure 7. Magnetized Threshold, Helium.

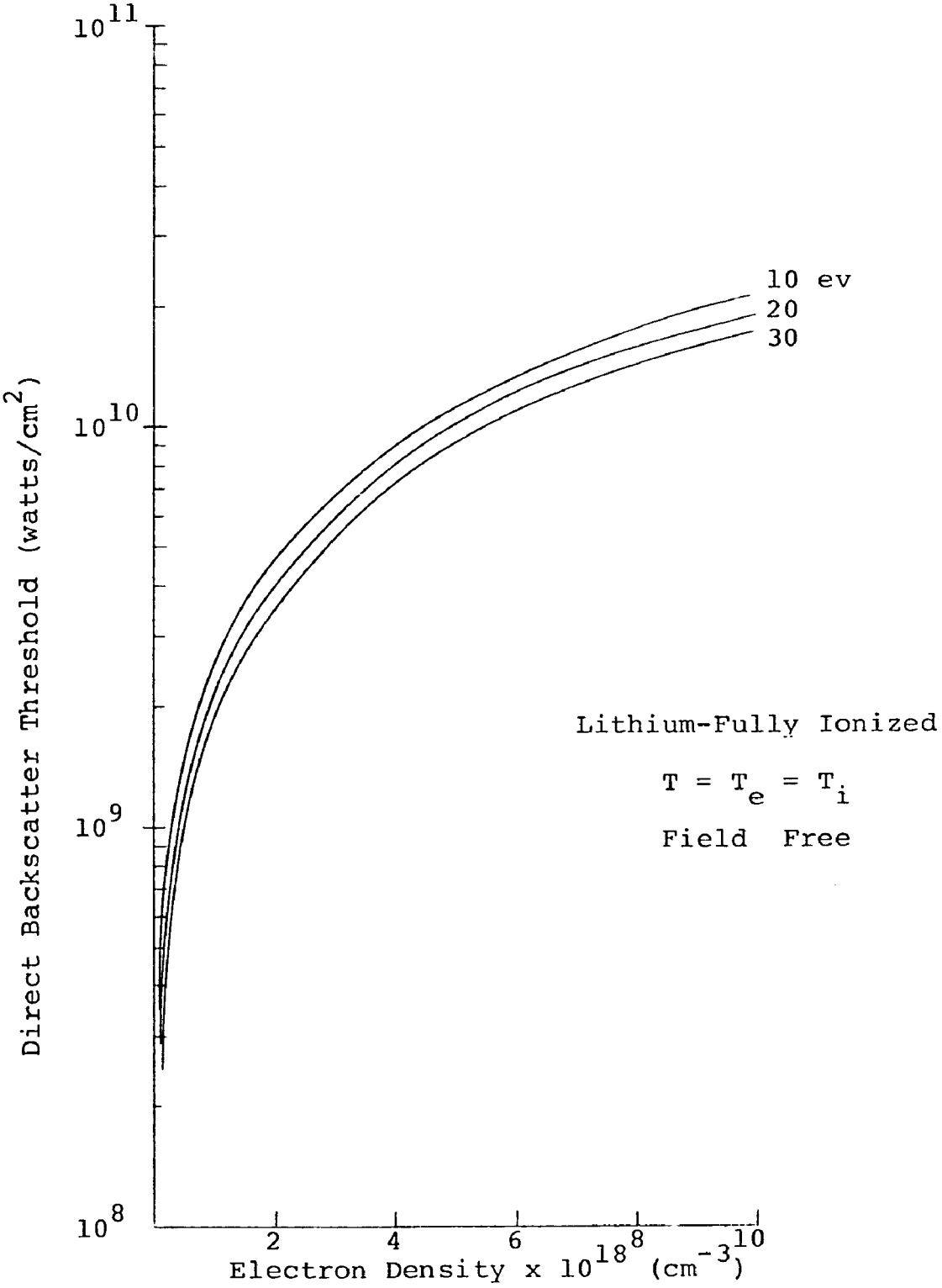


Figure 8. Field-Free Threshold, Lithium.

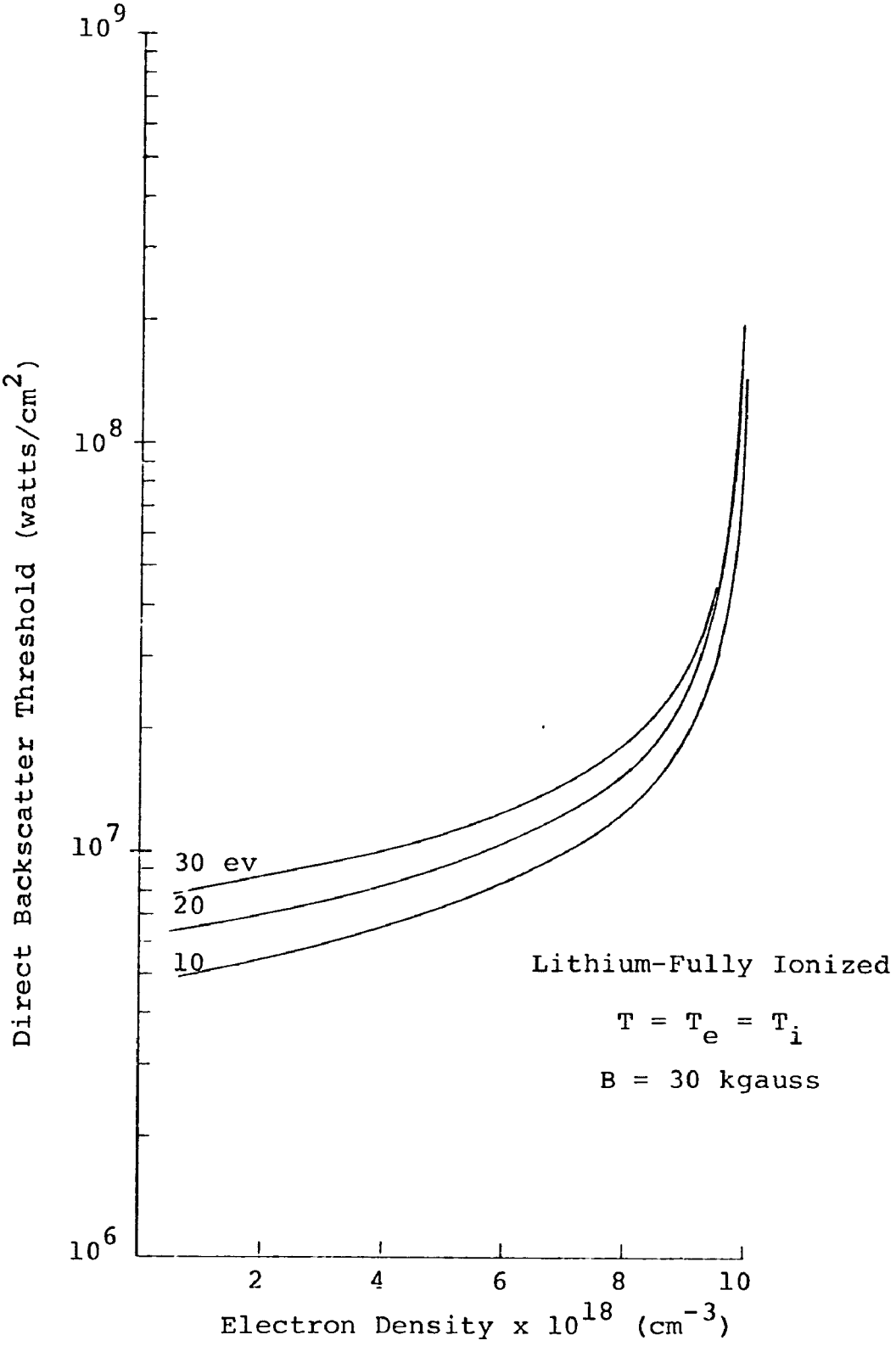


Figure 9. Magnetized Threshold, Lithium.

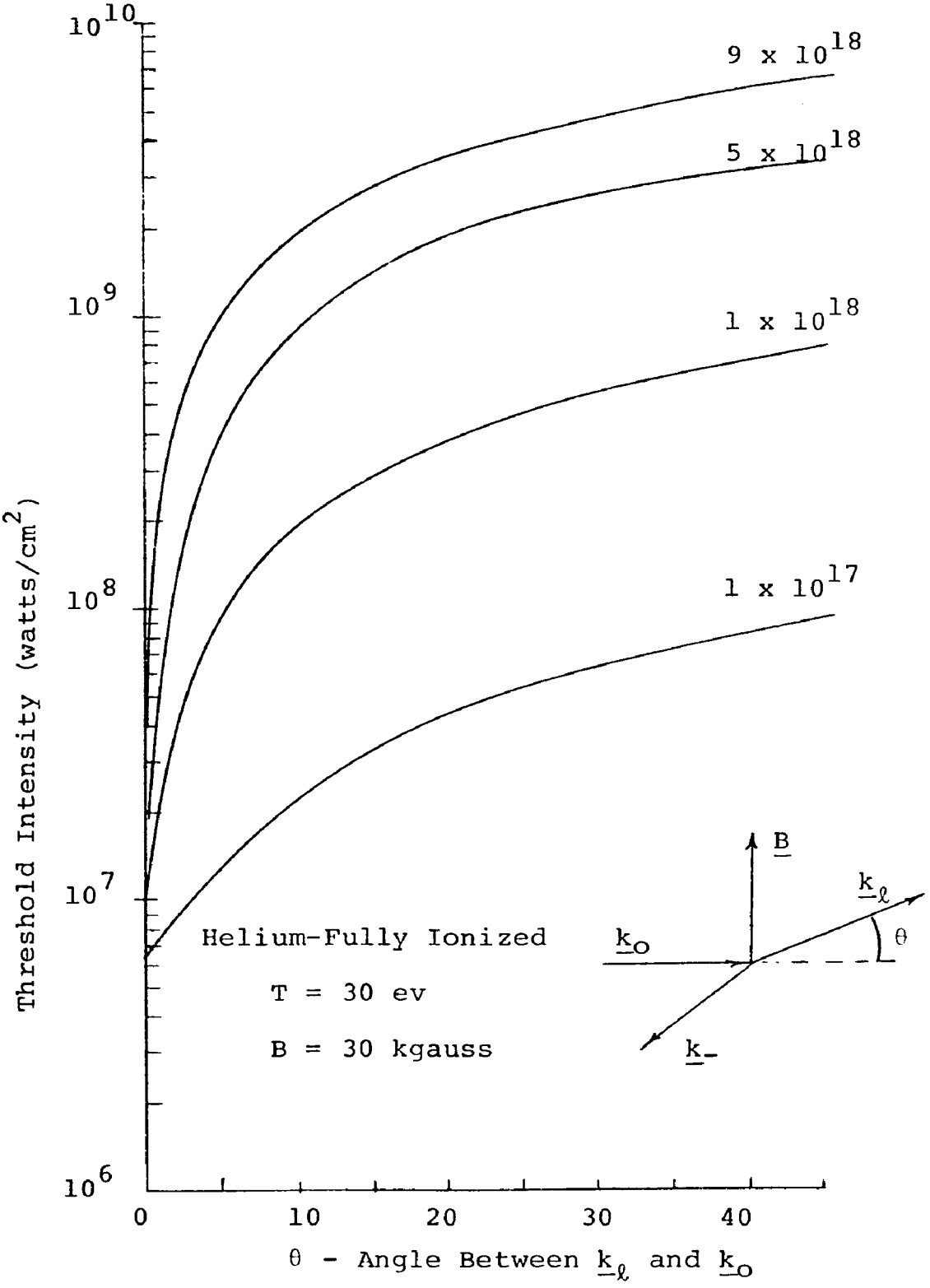


Figure 10. Magnetized Threshold vs Angle, Helium.

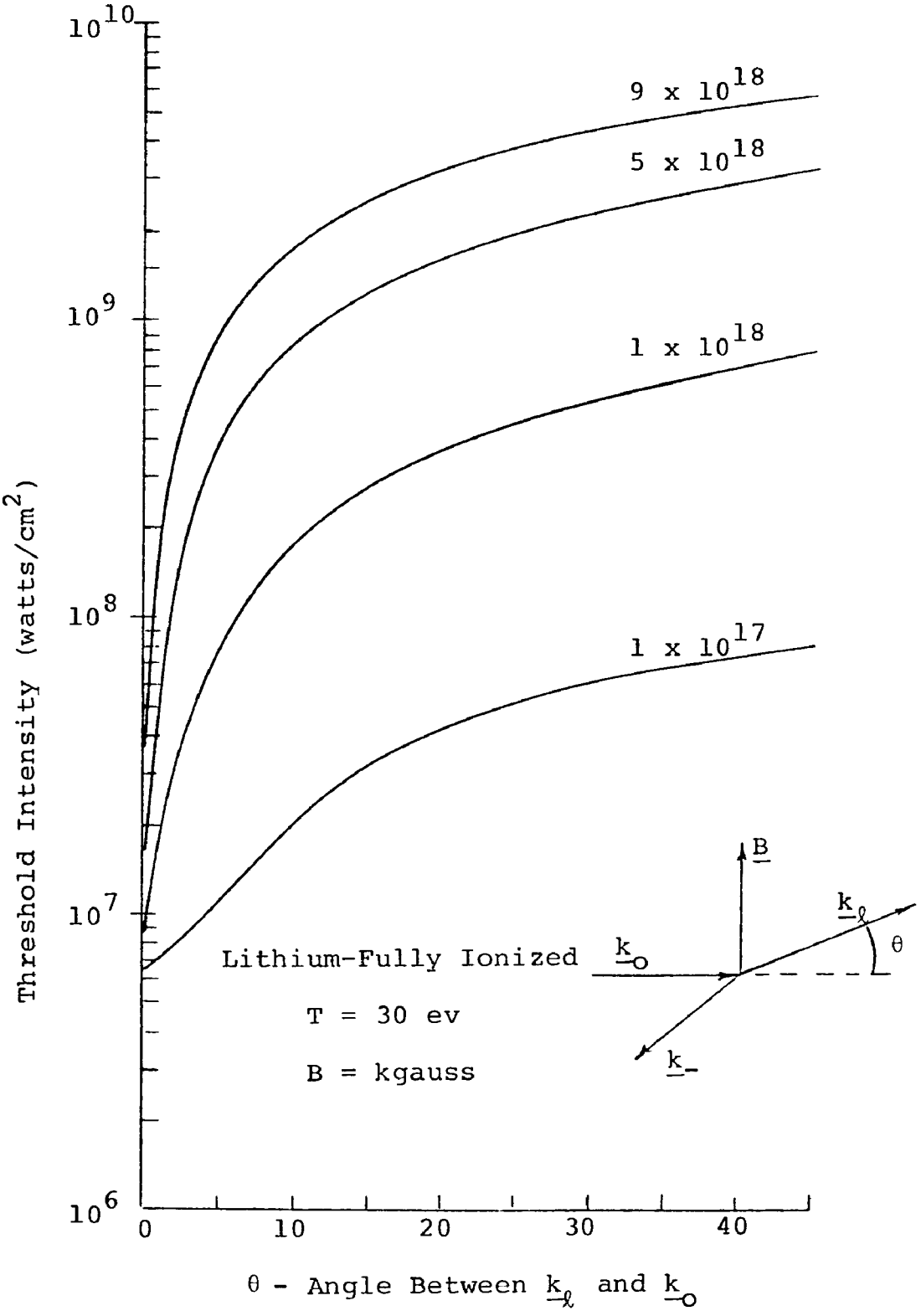


Figure 11. Magnetized Threshold vs Angle, Lithium.

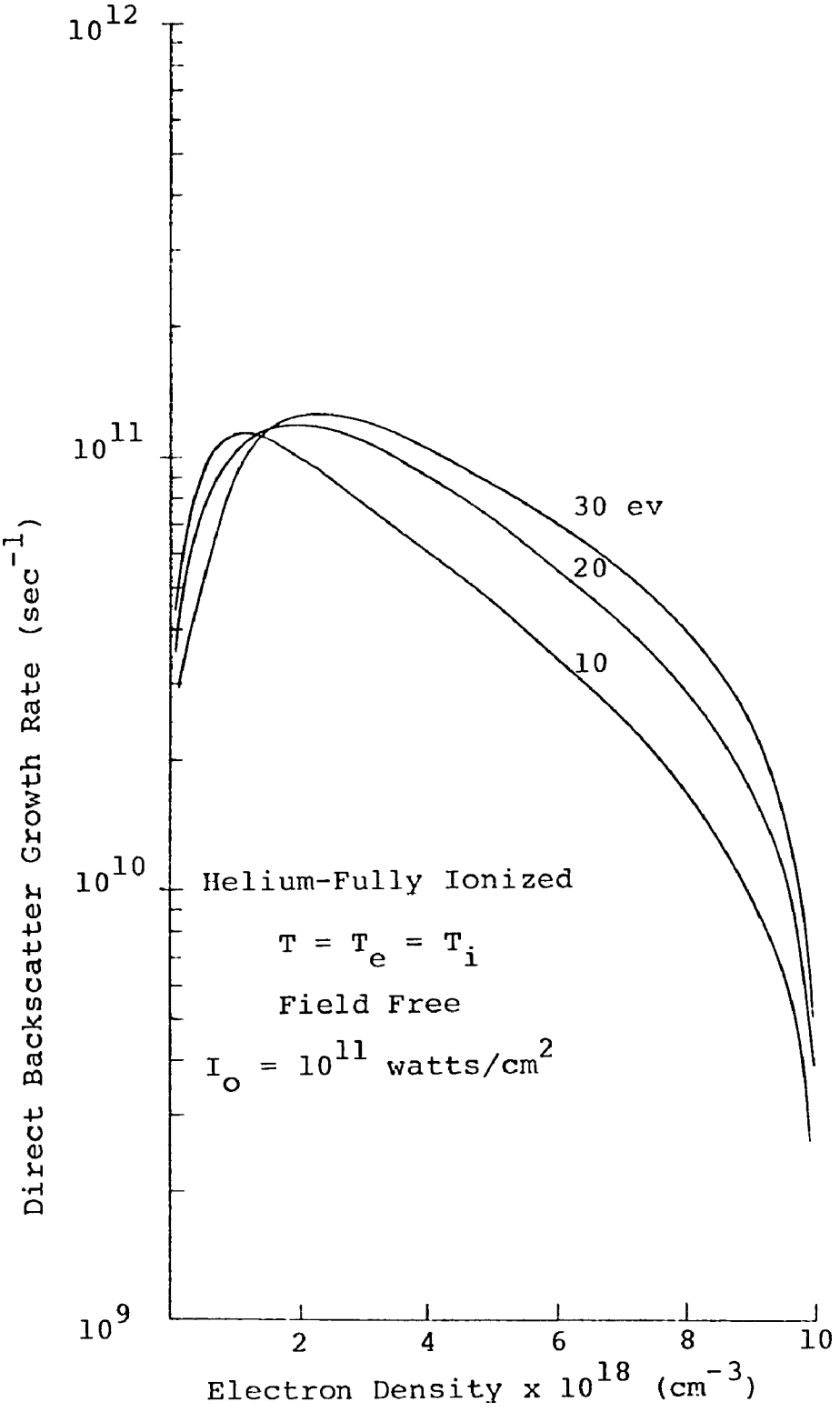


Figure 12. Field-Free Growth Rate, Helium.

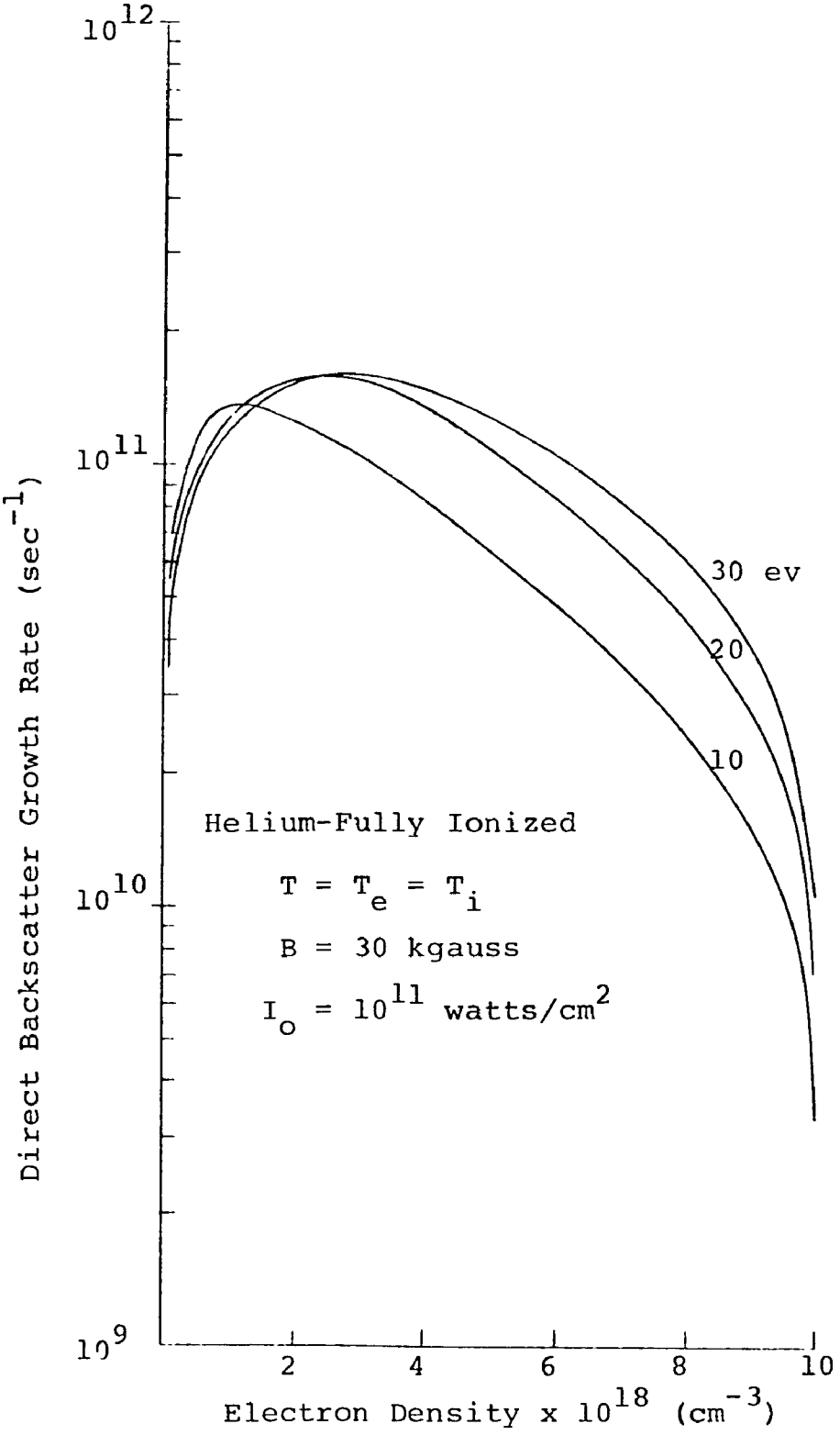


Figure 13. Magnetized Growth Rate, Helium

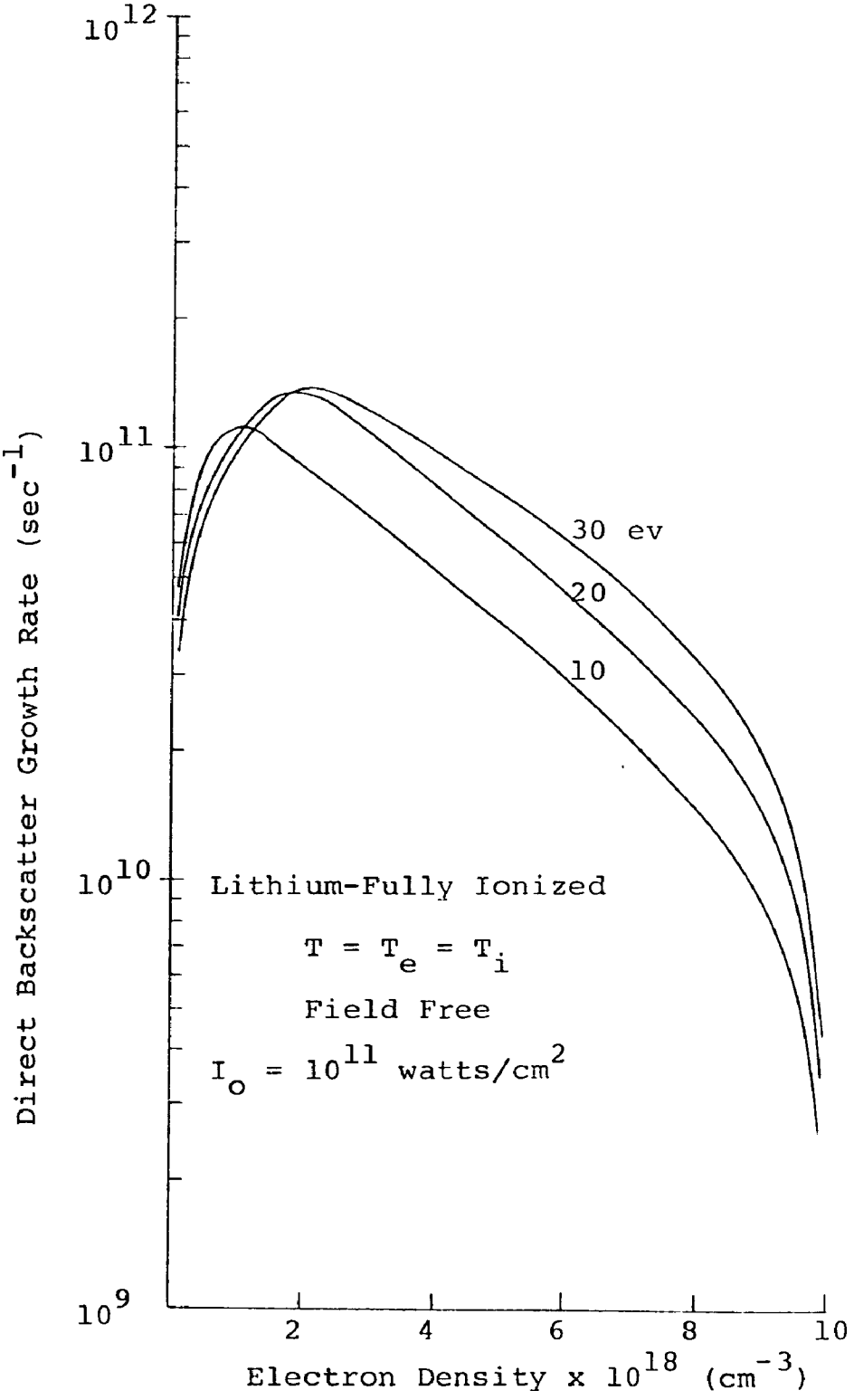


Figure 14. Field-Free Growth Rate, Lithium.

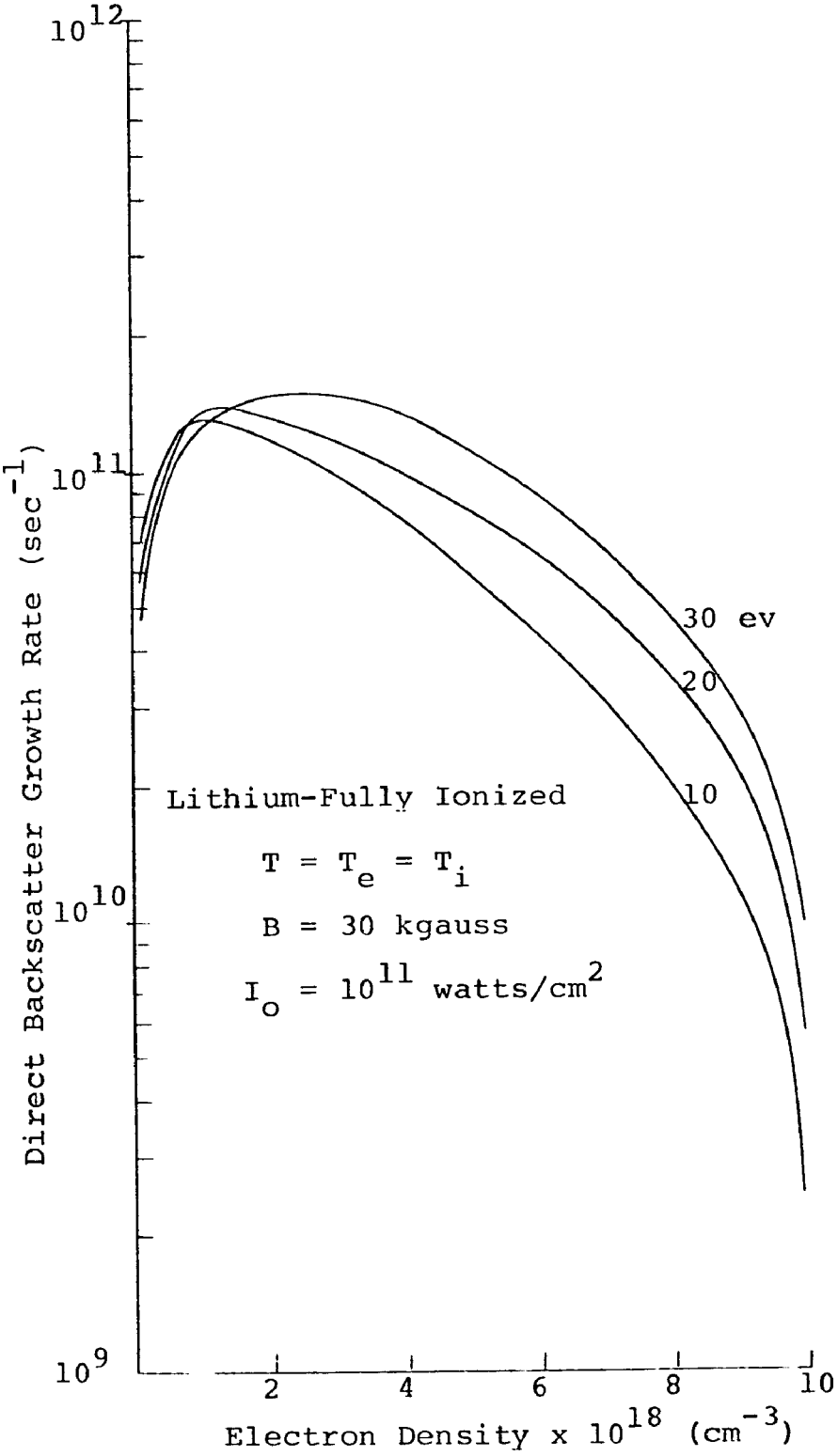


Figure 15. Magnetized Growth Rate, Lithium.

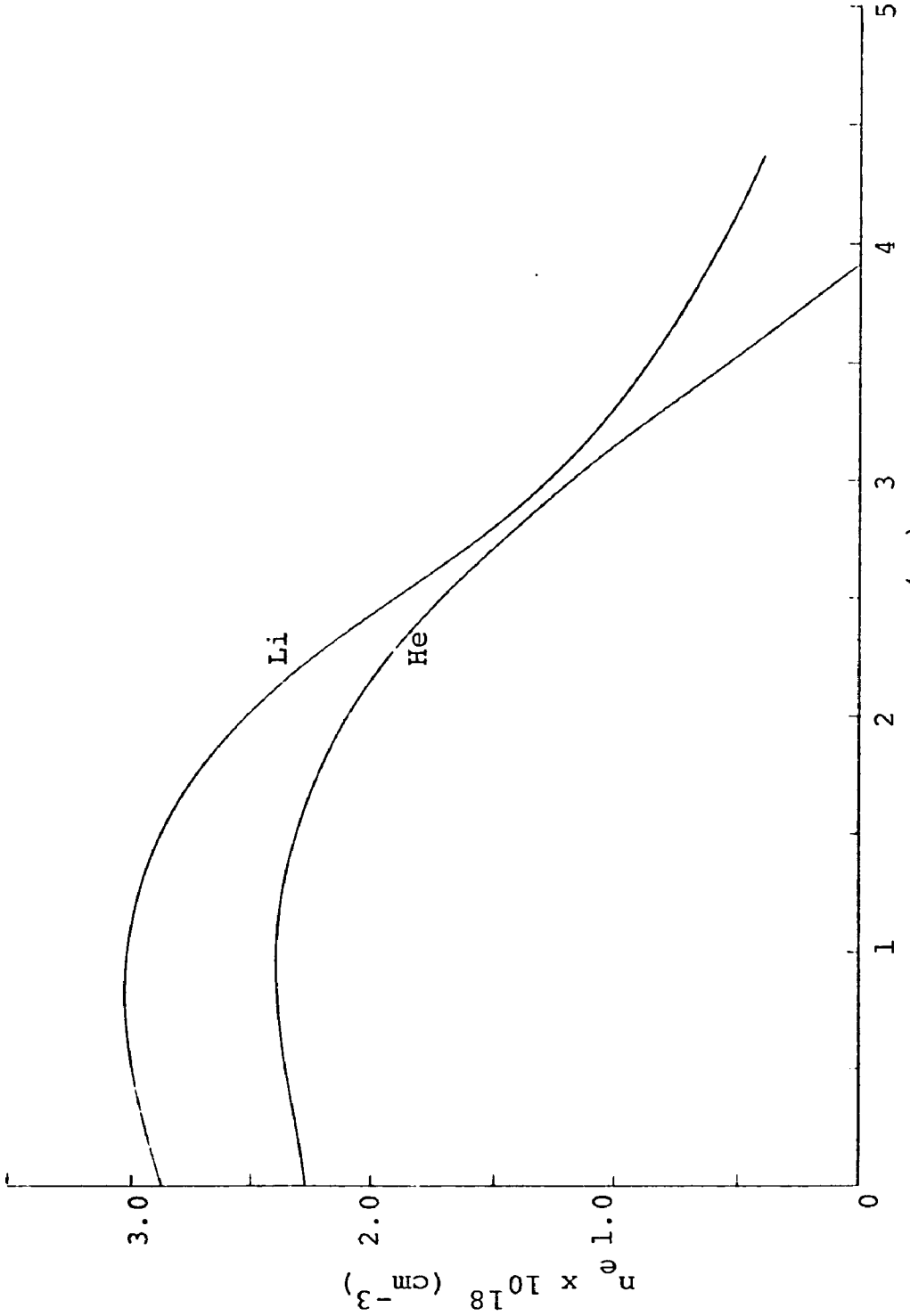


Figure 16. Radial Density Profile

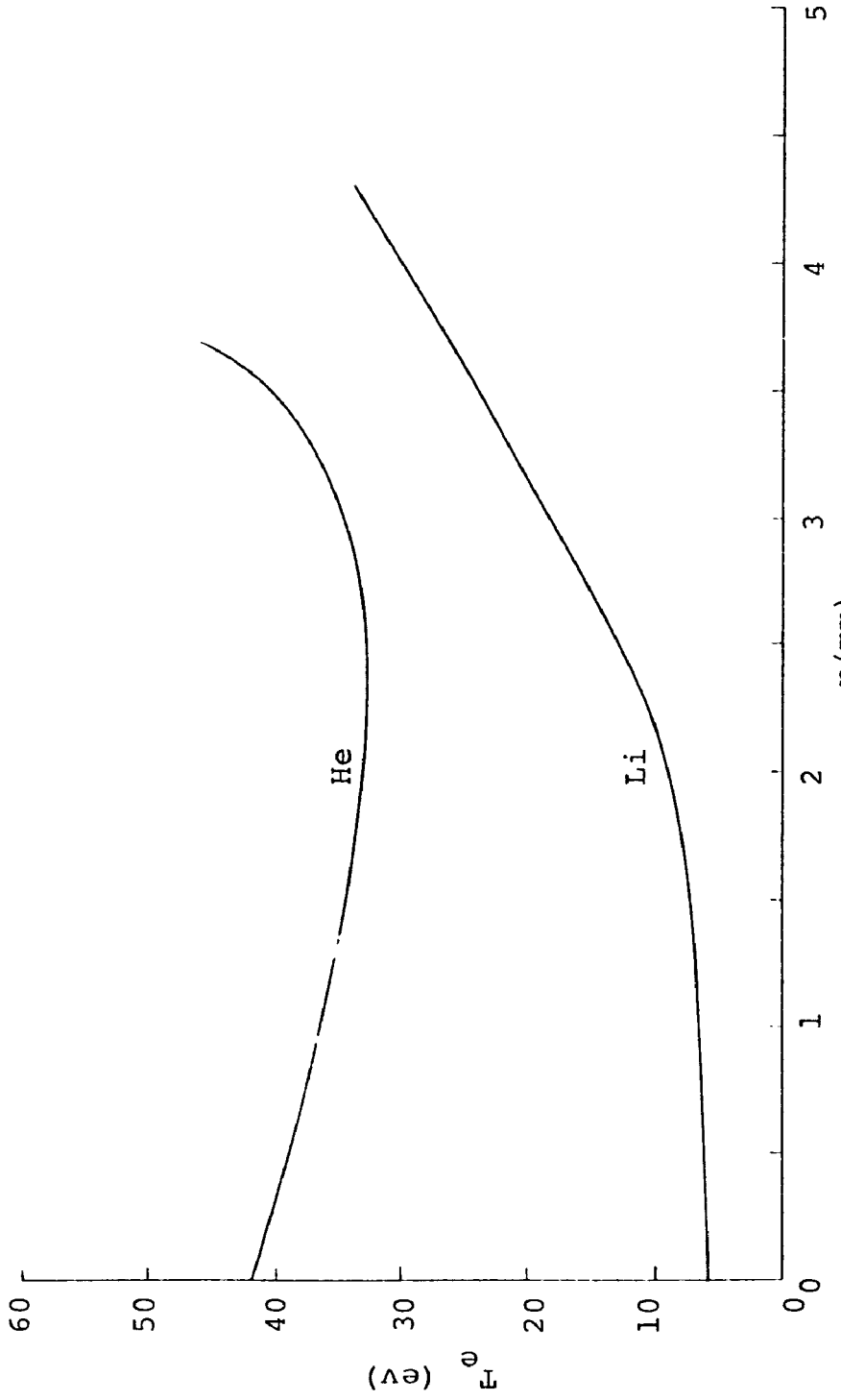


Figure 17. Radial Temperature Profile.

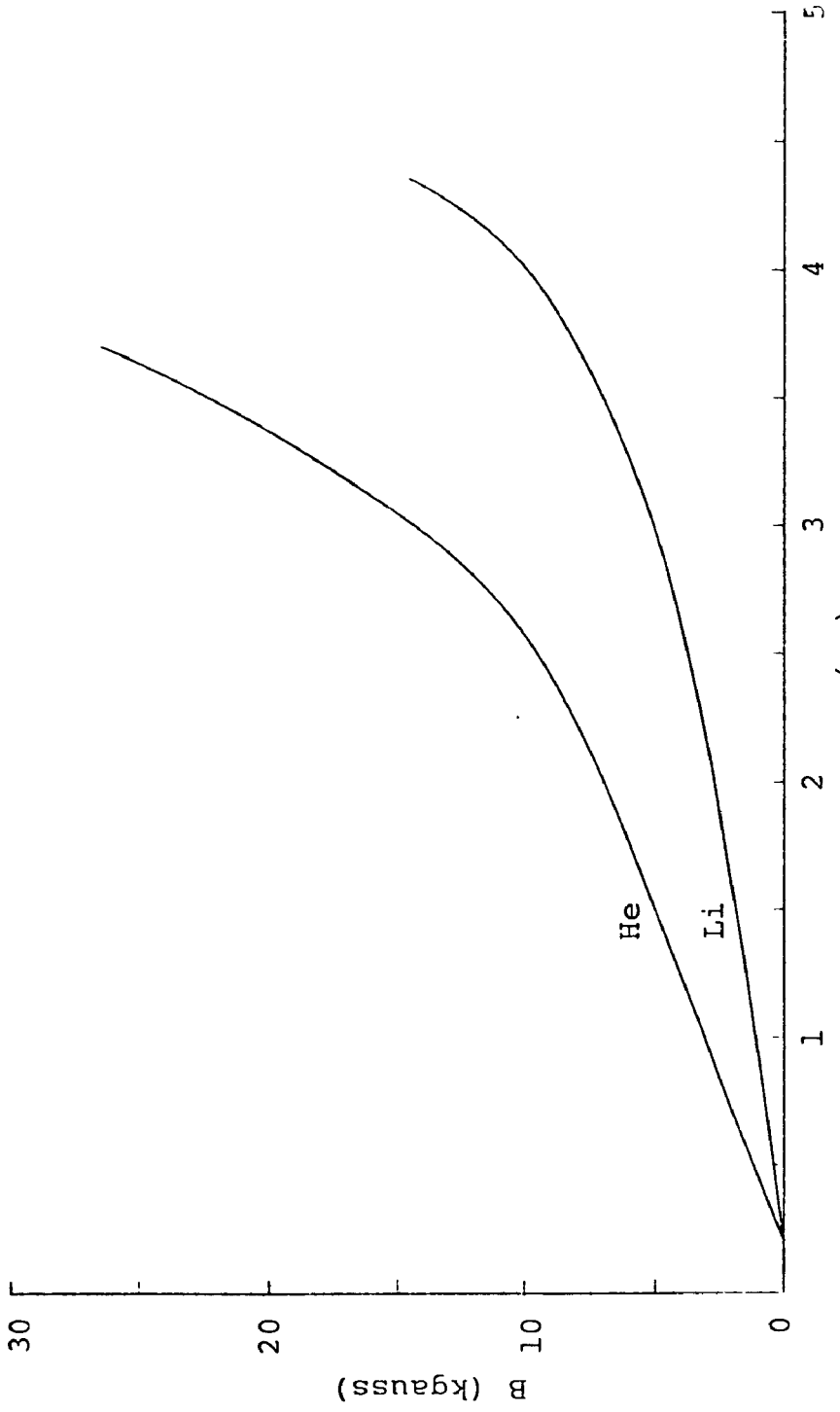


Figure 18. Radial Magnetic Field Profile.

TABLE 4. e-FOLDINGS IN HELIUM Z-PINCH

Helium Z-Pinch, $I_o = 10^{11}$ watts/cm^2

r (mm)	Backscatter		Sidescatter	
	Equation No.	e-foldings	Equation No.	e-foldings
.5	4.4	20.4	4.4	18.9
1.2	4.7	41.7	4.5	82.5
1.5	4.7	45.7	4.4	28.4
1.7	4.7	46.3	4.4	28.3
2.1	4.7	74.9	4.4	28.0
2.4	4.7	82.9	4.4	27.7
2.6	4.7	46.6	4.4	26.6
2.8	4.7	26.3	4.4	23.7
3.2	4.7	11.1	4.5	36.2
3.6	4.7	3.4	4.5	7.9

Note: For r = .5 mm the magnetic field is very small. As a result, field free equations were used.

TABLE 5. e-FOLDINGS IN LITHIUM Z-PINCH

Lithium Z-Pinch, $I_o = 10^{11}$ watts/cm^2

r (mm)	Backscatter		Sidescatter	
	Equation No.	e-foldings	Equation No.	e-foldings
.38		0		0
.92	4.7	14.4		0
1.2	4.7	9.3		0
1.5	4.7	9.5		0
1.7	4.7	10.0	4.5	15.4
2.0	4.7	9.4	4.5	15.6
2.3	4.7	10.8	4.5	19.2
2.8	4.7	10.2	4.5	19.3
3.4	4.7	8.8	4.5	17.5
4.3	4.7	5.1	4.5	10.4

Note: For r = .38 mm the magnetic field is very small. As a result field free equations were used.

VI. CONCLUSIONS

This thesis has studied stimulated Brillouin scattering, a nonlinear pocess important in laser-plasma interactions. All important effects such as magnetic fields, plasma temperature, arbitrary angle of propagation of the stimulated waves, boundedness, and inhomogeneities have been included in the investigation. This complete treatment allows a detailed analysis of experimental plasmas.

The following points unique to this thesis should be emphasized:

1. The dispersion relation describing stimulated Brillouin scattering has been obtained in a form that is the same as that derived by Nishikawa for coherent, three-wave interactions. Thus, the correspondence of SBS to the canonical treatment of Nishikawa has been pointed out. The dispersion relation is more clearly solved as a result.
2. Previous investigations of SBS has been restricted as regards to the plasma parameter β (Refs. 7, 19, 41) (ratio of thermal pressure to magnetic pressure) and the angle of propagation of the stimulated waves[16,27,41]. These restrictions have been removed so that the angles of each of the three waves with respect to the magnetic field in any warm plasma are arbitrary. As a result, this thesis is more general than the other treatments.

3. There are several modifications to field free SBS due to the inclusion of an imposed DC magnetic field in the dispersion relation. A magnetosonic mode of the plasma is driven across field lines in lieu of the ion acoustic wave. Because the damping rate of the high frequency Alfvén wave is lower than the damping rate of the ion acoustic wave ($T_i \simeq T_e$), the threshold of the instability is lower. The addition of the magnetic field inhomogeneity causes a larger wave vector mismatch than in the field free case. This inhibits growth of SBS in nonuniform plasmas because the waves more quickly convect out of the unstable region.
4. Stimulated Brillouin scattering should be readily observable in the Z-pinch experiment being conducted at The University of Michigan. The predicted number of exponentiations of the backscattered wave above the initial noise level should result in large percentages of backscattered radiation. Indeed, saturation of the instability by pump depletion[10] should occur. It should be noted that preliminary results from the experiment[34] at the time this thesis was written indicate that other anomalous processes may be competing with SBS. Their effects including modification of the plasma and refocusing of the laser are beyond the scope of this thesis.

APPENDIX A

Electron and Ion Conductivity

The dispersion relation for SBS, Eq. (3.1), contains the low frequency, linear electron and ion conductivities, $\underline{\underline{\sigma}}_e$ and $\underline{\underline{\sigma}}_i$. To solve the dispersion relation these must be derived. First, for the electrons the equations governing their motion are

$$\frac{\partial \underline{v}_e}{\partial t} + \underline{v}_e \cdot \nabla \underline{v}_e = - \frac{e}{m_e} \left(\underline{E} + \frac{\underline{v}_e \times \underline{B}_o}{c} \right) - \frac{T_e \nabla n_e}{n_e m_e} \tag{A.1}$$

$$\frac{\partial \underline{v}_e}{\partial t} + \nabla \cdot n_e \underline{v}_e = 0 \tag{A.2}$$

These equations are solved by linearizing and writing the perturbation terms in harmonic form. For example (hats indicate perturbation quantities),

$$n_e = n_o + \hat{n}_e \, e^{i(\underline{k} \cdot \underline{r} - \omega t)}$$

To first order the equations of motion [(A.1) and (A.2)] are

$$- i\omega \, \hat{\underline{v}}_e = - \frac{e}{m_e} \hat{\underline{E}} - \hat{\underline{v}}_e \times \underline{\omega}_{ce} - \frac{T_e}{n_o m_e} i\underline{k} \hat{n}_e$$

$$- i\omega \, \hat{n}_e + i n_o \underline{k} \cdot \hat{\underline{v}}_e = 0$$

where $\underline{\omega}_{ce} = (e\underline{B}_o / m_e c)$, $\underline{B}_o$ is the imposed field.

Combining the two above equations

$$- i\omega \underline{\hat{v}}_e - \underline{\omega}_{ce} \times \underline{\hat{v}}_e = - \frac{e}{m_e} \underline{\hat{E}} - \frac{T_e}{m_e} \frac{i\underline{k}(\underline{k} \cdot \underline{\hat{v}}_e)}{\omega} \qquad (A.3)$$

A coordinate system is chosen with $\underline{k}$ in the $\underline{Z}$-direction and $\underline{B}_o$ in the X-Z plane. Equation (A.3) written in component form is

$$- i\omega \hat{v}_{ex} + \omega_{cez} \hat{v}_{ey} = - \frac{e}{m_e} \hat{E}_x$$

$$- i\omega_{cez} \hat{v}_{ex} - i\omega \hat{v}_{ey} + \omega_{cex} \hat{v}_{ez} = - \frac{e}{m_e} \hat{E}_y$$

$$- \omega_{cex} \hat{v}_{ey} + i \left(\frac{T_e k^2}{\omega m_e} - \omega \right) \hat{v}_{ez} = - \frac{e}{m_e} \hat{E}_z$$

From these equations $\hat{v}_{ez}$, $\hat{v}_{ey}$ and $\hat{v}_{ez}$ are

$$\hat{v}_{ex} = - \frac{e}{m_e} \frac{1}{D_e} \left\{ \hat{E}_x \left(k^2 \frac{T_e}{m_e} - \omega^2 + \omega_{cex}^2 \right) \right.$$

$$\left. + \hat{E}_y \left[- i\omega_{cez} \left(\frac{T_e k^2}{\omega m_e} - \omega \right) \right] + \hat{E}_z \, \omega_{cex} \, \omega_{cez} \right\} \qquad (A.4)$$

$$\hat{v}_{ey} = - \frac{e}{m_e} \frac{1}{D_e} \left\{ \hat{E}_x \, i\omega_{cez} \left(\frac{T_e k^2}{\omega m_e} - \omega \right) + \hat{E}_y \left(\frac{k^2 T_e}{m_e} - \omega^2 \right) \right.$$

$$\left. + \hat{E}_z \, i\omega_{cex} \, \omega \right\} \qquad (A.5)$$

$$\hat{v}_{ez} = - \frac{e}{m_e} \frac{1}{D_e} \left\{ \hat{E}_x \, \omega_{cex} \, \omega_{cez} + \hat{E}_y \, (-i\omega\omega_{cex}) + \hat{E}_z \, (- \omega^2 + \omega_{cez}^2) \right\} \tag{A.6}$$

with

$$D_e = - i\omega \left(- \omega^2 + \omega_{cex}^2 + \omega_{cez}^2 + k^2 \frac{T_e}{m_e} \right) + i\omega_{cez}^2 \frac{k^2 T_e}{\omega m_e} \tag{A.7}$$

Since the electron current is

$$\underline{J}_e = - en_o \, \underline{\hat{v}}_e = \underline{\underline{\sigma}}_e \cdot \underline{\hat{E}} \tag{A.8}$$

the elements of the electron conductivity tensor can be written from Eqs. (A.4) to (A.6).

$$\sigma_{e_{11}} = (\omega_{pe}^2/4\pi) \, 1/D_e \, [k^2 \, (T_e/m_e) - \omega^2 + \omega_{cex}^2]$$

$$\sigma_{e_{12}} = - \sigma_{e_{21}} = - (i\omega_{pe}^2/4\pi)(\omega_{cez}/D_e)[(k^2 T_e/\omega m_e) - \omega]$$

$$\sigma_{e_{13}} = \sigma_{e_{31}} = (\omega_{pe}^2/4\pi)(\omega_{cex}\omega_{cez}/D_e)$$

$$\sigma_{e_{22}} = (\omega_{pe}^2/4\pi) \, 1/D_e \, [k^2 \, (T_e/m_e) - \omega]$$

$$\sigma_{e_{23}} = - \sigma_{e_{32}} = (i\omega_{pe}^2/4\pi)(\omega\omega_{cex}/D_e)$$

$$\sigma_{e_{33}} = (\omega_{pe}^2/4\pi) \, 1/D_e \, (\omega_{cez}^2 - \omega^2) \tag{A.9}$$

The equation of motion for the ions differs only by the sign of the charge, the mass, and the temperature.

$$\frac{\partial \underline{v}_i}{\partial t} + \underline{v}_i \cdot \nabla \underline{v}_i = \frac{e}{m_i}\left(\underline{E} + \frac{\underline{v}_i \times \underline{B}_o}{c}\right) - \frac{T_i \nabla n_i}{n_o m_i}$$

Following the steps above exactly the ion conductivity can be derived. Its form is the same as the electron conductivity except all quantities have the subscript for ions and the components of the cyclotron frequency have the opposite sign.

APPENDIX B

Formal Treatment of Dispersion Relation

The dispersion relation for SBS is given by Eq. (3.1) as

$$D = \frac{\underline{k}_\ell}{\omega_\ell} \cdot \underline{\underline{\sigma}}_e \cdot \underline{\underline{Q}} \cdot i\underline{k}_\ell \cdot \left(\frac{\omega_\ell^2}{c^2} \underline{\underline{I}} + \frac{4\pi i \omega_\ell}{c^2} \underline{\underline{\sigma}}_i \right) \frac{\omega_{pe}^2}{m_e n_o \omega_o^2 c^2} \frac{|E_o^{t-}|^2}{D_-^t} \qquad (B.1)$$

with

$$D_-^t = \frac{\omega_-^2}{c^2} - \underline{k}_- \cdot \underline{k}_- - \frac{\omega_{pe}^2}{c^2}$$

$$|E_o^{t-}|^2 = \sin^2\psi \; E_o^2$$

ψ = the angle between $\underline{k}_-$ and $\underline{E}_o$

$D = \det \underline{\underline{K}}$

$\underline{\underline{Q}}$ = matrix of cofactors of $\underline{\underline{K}}$ transpose

$$\underline{\underline{K}} = - \underline{k}_\ell \times \underline{k}_\ell \times \underline{\underline{I}} - \frac{\omega_\ell^2}{c^2} \underline{\underline{I}} - \frac{4\pi i \omega_\ell}{c^2} (\underline{\underline{\sigma}}_e + \underline{\underline{\sigma}}_i)$$

This dispersion relation can be expanded formally by deriving D and $\underline{\underline{Q}}$ from $\underline{\underline{K}}$ and simplifying. Since

$$\sigma_{j_{12}} = - \sigma_{j_{21}}, \; \sigma_{j_{13}} = \sigma_{j_{31}}, \text{ and } \sigma_{j_{23}} = - \sigma_{j_{32}}$$

where j stands for e and i,

$$K_{12} = - K_{21}, \; K_{13} = K_{31} \text{ and } K_{32} = - K_{23}.$$

Thus

$$D = \det \underline{\underline{K}} = K_{11}(K_{22}K_{33} + K_{23}^2) + K_{12}(K_{12}K_{33} + K_{13}K_{23}) + K_{13}(K_{12}K_{23} - K_{22}K_{13}) \tag{B.2}$$

$\underline{\underline{Q}}$ is the matrix of cofactors of $\underline{\underline{K}}$ transpose.

$$\underline{\underline{Q}} = \begin{bmatrix} K_{22}K_{33} + K_{23}^2 & -K_{12}K_{33} - K_{13}K_{23} & K_{12}K_{23} - K_{13}K_{22} \\ K_{12}K_{33} + K_{13}K_{23} & K_{11}K_{33} - K_{13}^2 & -K_{11}K_{23} - K_{12}K_{13} \\ K_{12}K_{23} - K_{13}K_{22} & K_{11}K_{23} + K_{12}K_{13} & K_{11}K_{22} + K_{12}^2 \end{bmatrix} \tag{B.3}$$

So

$$D = K_{11}Q_{11} + K_{12}Q_{21} + K_{13}Q_{31} \tag{B.4}$$

The right side of (B.1) can be simplified in the chosen coordinate system, $\underline{k}_\ell = [0,0,k_\ell]$. Combining Eqs. (B.4) and (B.5), Eq. (B.6) becomes the dispersion relation. $\underline{\underline{Q}}$ is given by Eq. (B.3), $\underline{\underline{g}}_e$ by Eq. (A.10) and $\underline{\underline{g}}_i$ by Eq. (A.11). Equation (B.6) is the starting point for the calculations in Chapter III. [Equation (B.5) appears on next page.]

Unfortunately this form is still too complicated to draw any general conclusions. It is interesting, however, to consider the case $\underline{k}_\ell \| \underline{B}_o$ ($\phi_\ell = 0$) since it can be solved without any assumptions concerning the relative magnitudes of ω_ℓ and ω_{ci}. As mentioned in Chapter III, when aligned with the external field, the instability is unaffected by the field, and the field free results are recovered.

$$\frac{\underline{k}_\ell}{\omega_\ell}\cdot\underline{\underline{\sigma}}_e\cdot\underline{\underline{Q}}\cdot i\underline{k}_\ell\cdot\left(\frac{\omega_\ell^2}{c^2}\,\underline{\underline{I}}+\frac{4\pi i\omega_\ell}{c^2}\,\underline{\underline{\sigma}}_i\right)$$

$$=\left[0,0,\frac{k_\ell}{\omega_\ell}\right]\cdot\begin{bmatrix}\sigma_{e_{11}} & \sigma_{e_{12}} & \sigma_{e_{13}}\\ \sigma_{e_{21}} & \sigma_{e_{22}} & \sigma_{e_{23}}\\ \sigma_{e_{31}} & \sigma_{e_{32}} & \sigma_{e_{33}}\end{bmatrix}\cdot\begin{bmatrix}Q_{11} & Q_{12} & Q_{13}\\ Q_{21} & Q_{22} & Q_{23}\\ Q_{31} & Q_{32} & Q_{33}\end{bmatrix}\cdot[0,0,k_\ell]$$

$$\cdot\begin{bmatrix}\frac{\omega_\ell^2}{c^2}+\frac{4\pi i\omega_\ell}{c^2}\sigma_{i_{11}} & \frac{4\pi i\omega_\ell}{c^2}\sigma_{i_{12}} & \frac{4\pi i\omega_\ell}{c^2}\sigma_{i_{13}}\\ \frac{4\pi i\omega_\ell}{c^2}\sigma_{i_{21}} & \frac{\omega_\ell^2}{c^2}+\frac{4\pi i\omega_\ell}{c^2}\sigma_{i_{22}} & \frac{4\pi i\omega_\ell}{c^2}\sigma_{i_{23}}\\ \frac{4\pi i\omega_\ell}{c^2}\sigma_{i_{31}} & \frac{4\pi i\omega_\ell}{c^2}\sigma_{i_{32}} & \frac{\omega_\ell^2}{c^2}+\frac{4\pi i\omega_\ell}{c^2}\sigma_{i_{33}}\end{bmatrix}$$

$$=-\frac{4\pi k_\ell^2}{c^2}\left\{\sigma_{e_{31}}\left[Q_{11}\,\sigma_{i_{31}}+Q_{12}\,\sigma_{i_{32}}+Q_{13}\left(\frac{\omega_\ell}{4\pi i}+\sigma_{i_{33}}\right)\right]\right.$$

$$+\sigma_{e_{32}}\left[Q_{21}\,\sigma_{i_{31}}+Q_{22}\,\sigma_{i_{32}}+Q_{23}\left(\frac{\omega_\ell}{4\pi i}+\sigma_{i_{33}}\right)\right]$$

$$\left.+\sigma_{e_{33}}\left[Q_{31}\,\sigma_{i_{31}}+Q_{32}\,\sigma_{i_{32}}+Q_{33}\left(\frac{\omega_\ell}{4\pi i}+\sigma_{i_{33}}\right)\right]\right\}$$

(B.5)

$$K_{11}Q_{11} + K_{12}Q_{21} + K_{13}Q_{31} = - \frac{4\pi k_\ell^2}{c^2} \left\{ \sigma_{e_{31}} \left[Q_{11}\, \sigma_{i_{31}} + Q_{12}\, \sigma_{i_{32}} + Q_{13} \left(\frac{\omega_\ell}{4\pi i} + \sigma_{i_{33}} \right) \right] \right.$$

$$+ \sigma_{e_{32}} \left[Q_{21}\, \sigma_{i_{31}} + Q_{22}\, \sigma_{i_{32}} + Q_{23} \left(\frac{\omega_\ell}{4\pi i} + \sigma_{i_{33}} \right) \right]$$

$$\left. + \sigma_{e_{33}} \left[Q_{31}\, \sigma_{i_{31}} + Q_{32}\, \sigma_{i_{32}} + Q_{33} \left(\frac{\omega_\ell}{4\pi i} + \sigma_{i_{33}} \right) \right] \right\} \quad \text{(B.6)}$$

For $\underline{k} \,||\, \underline{B}_o$, $\omega_{cix} = \omega_{cex} = 0$, so the following terms are all zero: $\sigma_{j_{13}}$, $\sigma_{j_{31}}$, $\sigma_{j_{23}}$, $\sigma_{j_{32}}$, K_{13}, K_{23}, K_{31}, K_{32}, Q_{13}, Q_{23}, Q_{31} and Q_{32}. $\underline{Q}$ becomes equal to

$$\underline{Q} = \begin{bmatrix} K_{22}K_{33} & - K_{12}K_{33} & 0 \\ K_{12}K_{33} & K_{11}K_{33} & 0 \\ 0 & 0 & K_{11}K_{22} + K_{12}^2 \end{bmatrix}$$

and the dispersion relation (B.6) simplifies to

$$K_{33}(K_{11}K_{22} + K_{12}^2) = - \frac{4\pi k_\ell^2}{c^2} \sigma_{e_{33}} (K_{11}K_{22} + K_{12}^2) \left(\frac{\omega_\ell}{4\pi i} + \sigma_{i_{33}} \right)$$

$$\times \frac{\omega_{pe}^2}{m_e n_o \omega_o^2 c^2} \frac{\sin^2\psi\, E_o^2}{D_-^t}$$

Cancelling common terms and assuming $\omega_\ell << \omega_{pi}$, ω_{ce}, and $k_\ell^2 (T_e/m_e)$

$$K_{33} = - \frac{\omega_{pi}^2}{c^2 k_\ell^2} \frac{(\omega_\ell^2 - k_\ell^2 c_s^2)}{c_s^2}$$

and the dispersion relation is

$$- \frac{\omega_{pi}^2}{c^2 k_\ell^2} \frac{(\omega_\ell^2 - k_\ell^2 c_s^2)}{c_s^2} = - \frac{4\pi k_\ell^2}{c^2} \frac{\omega_{pe}^2}{4\pi i} \frac{\omega_\ell}{k_\ell^2 (T_e/m_e)} \frac{\omega_{pi}^2}{4\pi i \omega_\ell}$$

$$\frac{\omega_{pe}^2}{m_e n_o \omega_o^2 c^2} \frac{\sin^2\psi \; E_o^2}{D_-^2}$$

or

$$(\omega_\ell^2 - k_\ell^2 c_s^2) \; D_-^t + \frac{k_\ell^2 \omega_{pi}^2 e^2 \sin^2\psi \, E_o^2}{\omega_o^2 m_e} = 0$$

So the coupling coefficient,

$$K = \frac{k_\ell^2 \omega_{pi}^2 e^2 \sin^2\psi \; E_o^2}{\omega_o^2 m_e^2}$$

is the same as in Chapter III. Since $\omega_\ell = k_\ell c_s$, the ion acoustic wave which is unmodified for propagation along magnetic field lines is the low frequency component of SBS. The low frequency modes with transverse polarization

$$\omega_\ell^2 = k_\ell^2 c_a^2 \qquad (\omega_\ell^2 << \omega_{ci}^2)$$

$$\omega_\ell^2 = \omega_{ci}^2 \left(1 - \frac{2\omega_{ci}^2}{c_a^2 k_\ell^2}\right) \qquad (\omega_\ell^2 \simeq \omega_{ci}^2)$$

$$\omega_\ell^2 = \frac{c_a^4 k_\ell^4}{\omega_{ci}^2} \qquad (\omega_\ell^2 >> \omega_{ci}^2)$$

are not excited. This is identical to the results of Drake et al.[7], and reproduces simply the work of Shukla et al.[27].

APPENDIX C

Linear Damping Rates

Expressions for the linear damping rates, Γ_ℓ and Γ_-, are needed to evaluate the thresholds and growth rates for specific plasmas. They are derived in this appendix.

C.1 For the backscattered electromagnetic wave ω_-, the dispersion relation including collisions is[36]

$$k^2c^2 = \omega^2 - \frac{\omega_{pe}^2}{1 + \frac{i\nu_{ei}}{\omega}}$$

$$\simeq \omega^2 - \omega_{pe}^2\left(1 - i\,\frac{\nu_{ei}}{\omega}\right)$$

for $$\nu_{ei} << \omega$$

ω can be separated into real and imaginary parts.

$$\omega = \omega_r - i\omega_i$$

Assuming $\omega_i << \omega_r$, the real part is

$$\omega_r^2 = k^2c^2 + \omega_{pe}^2 \qquad (C.1)$$

and the imaginary part is

$$\omega_i = \frac{\nu_{ei}}{2}\,\frac{\omega_{pe}^2}{(k^2c^2 + \omega_{pe}^2)} \qquad (C.2)$$

the frequencies are high enough that they are unaffected by the magnetic field.

C.2 For the ion acoustic wave in unmagnetized plasmas, damping is primarily due to Landau damping[14]. So

$$\omega_i = \frac{kc_s\sqrt{\pi/8}}{(1 + k^2\lambda_{D_e}{}^2)^{3/2}}\left\{\left(\frac{T_e}{T_i}\right)^{3/2} \exp\left[\frac{-T_e/T_i}{2(1 + k^2\lambda_{D_e}{}^2)}\right] + \sqrt{\frac{m_e}{m_i}}\right\}$$

In magnetized plasmas the mechanism of Landau damping is less effective for waves propagating obliquely to magnetic field lines. Indeed, if $\underline{k} \perp \underline{B}_o$, there is no Landau damping, and collisional damping is important. A correction must be made to Landau damping for oblique propagation, and the effects of collisions on the ion acoustic wave must be calculated.

Concerning Landau damping, when $\underline{k}$ has a component along the field lines, the free motion of the particles in that direction enables particle-wave resonance to occur. The criterion for significant damping is[5]

$$\cos\phi^2 > \frac{\omega^2}{k^2}\,(m_e/T_e) \qquad (C.3)$$

If this condition is met, the component of $\underline{k}$ along $\underline{B}_o$ is used in the Landau damping equation

$$\omega_i = \frac{k\cos\phi\ \ c_s\sqrt{\pi/8}}{(1 + k^2\lambda_{D_e}{}^2)}\left\{\left(\frac{T_e}{T_i}\right)^{3/2} \exp\left[\frac{-T_e/T_i}{2(1 + k^2\lambda_{D_e}{}^2)}\right] + \sqrt{\frac{m_e}{m_i}}\right\} \qquad (C.4)$$

Effectively Landau damping is reduced by $\cos\phi$ for ion acoustic waves propagating at an angle to $\underline{B}_o$. Since $\omega^2 = c_s{}^2k^2 \simeq (T_e/m_i)\,k^2$, condition (C.3) becomes

$$\cos^2 \phi > m_e/m_i$$

which is the same as the condition given in Chapter III for ion acoustic wave involvement in SBS.

The effect of collisions on the ion acoustic wave can be determined by the same method used to derive the conductivity tensor in Appendix A. Consider the electron momentum equation with a collision term added

$$\frac{\partial \underline{v}_e}{\partial t} + \underline{v}_e \cdot \nabla \underline{v}_e = - \frac{\nabla (n_e T_e)}{n_o m_e} - \nu_{ei} \underline{v}_e$$

Using normal mode analysis with $\underline{k}$ in the $\underline{Z}$-direction, the electron conductivity tensor $\underline{\underline{\sigma}}_e$ is

$$\underline{\underline{\sigma}}_e = \frac{\omega_{pe}^2}{4\pi} \begin{bmatrix} \frac{1}{i\omega - \nu_{ei}} & 0 & 0 \\ 0 & \frac{1}{i\omega - \nu_{ei}} & 0 \\ 0 & 0 & \frac{1}{i\omega - \nu_{ei} - \frac{ik^2 T_e}{\omega m_e}} \end{bmatrix}$$

For cold ions the conductivity tensor $\underline{\underline{\sigma}}_i$ is

$$\underline{\underline{\sigma}}_i = \frac{i\omega_{pi}^2}{4\pi\omega} \underline{\underline{I}}$$

$\underline{\underline{K}}$ was defined as

$$\underline{\underline{K}} = \underline{k} \times \underline{k} \times \underline{\underline{I}} - \frac{\omega^2}{c^2} \underline{\underline{I}} - \frac{4\pi i\omega}{c^2} (\underline{\underline{\sigma}}_e + \underline{\underline{\sigma}}_i)$$

Setting det $\underline{\underline{K}} = 0$ with $\underline{\underline{\sigma}}_e$ and $\underline{\underline{\sigma}}_i$ above gives

$$\omega^2 + i\nu_{ei} \frac{\omega_{pi}^2}{\omega_{pe}^2} \omega - k^2 c_s^2 = 0$$

Writing $\omega = \omega_r - i\omega_i$ and assuming $\omega_i << \omega_r$ the equations for the real and imaginary parts are

$$\omega_r = kc_s \tag{C.5}$$

$$\omega_i = \frac{\nu_{ei}}{2} \frac{\omega_{pi}^2}{\omega_{pe}^2} \tag{C.6}$$

The total ion acoustic damping rate is the sum of Eqs. (C.4) and (C.6).

$$\omega_i = \frac{\nu_{ei}}{2} \frac{\omega_{pi}^2}{\omega_{pe}^2} + \frac{k \cos\phi \, c_s \sqrt{\pi/8}}{(1 + k^2\lambda_{D_e}^2)^{3/2}}$$

$$\times \left\{ \left(\frac{T_e}{T_i}\right)^{3/2} \exp\left[\frac{-T_e/T_i}{(1 + k^2\lambda_{D_e}^2)}\right] + \sqrt{\frac{m_e}{m_i}} \right\} \tag{C.7}$$

C.3 When the low frequency wave excited by SBS propagates across the magnetic field ($\phi \approx \pi/2$), Landau damping is insignificant ($\cos\phi < m_e/m_i$). The damping of this mode, the high frequency Alfvén wave, is primarily due to collisions. The damping rate could be derived by considering an electron conductivity tensor which includes the effects of electron-ion collisions. However, it is easier to modify the dispersion relation of Stringer[35].

$$\left(\cos^2\phi - \frac{\omega^2}{k^2 c_a^2}\,Q\right)\left[\left(\cos^2\phi - \frac{\omega^2}{k^2 c_a^2}\right) - \frac{\omega^2}{k^2 c_a^2}\,Q\left(1 - \frac{\omega^2}{k^2 c_s^2}\right)\right]$$

$$= \frac{\omega^2}{\omega_{ci}^2}\cos^2\phi\left(1 - \frac{\omega^2}{k^2 c_s^2}\right) \qquad \text{(C.8)}$$

where

$$Q = 1 + \frac{k^2 c^2}{\omega_{pe}^2}$$

Collisions can be introduced through a finite resistivity term in Ohm's law. The one fluid equations of motion as given by Spitzer[28] are

$$\rho_o \frac{\partial \underline{v}}{\partial t} = -\nabla p + \underline{j} \times \underline{B}_o$$

$$\frac{m_e c}{n_o e^2}\frac{\partial \underline{j}}{\partial t} = \underline{E} + \frac{1}{c}\,\underline{v} \times \underline{B}_o - \frac{1}{n_o e}\,\underline{j} \times \underline{B}_o + \frac{1}{n_o e}\nabla p_e - \eta \underline{j}$$

where

$$\eta = \frac{\nu_{ei} m_e c}{n_o e^2}$$

introduces collisions. These are solved along with a continuity equation, the ideal gas law and Maxwell's equations. The derivatives are taken assuming variations as exp $i(\underline{k}\cdot\underline{r} - \omega t)$. After much manipulation the following equation is derived.

$$\left(1 + \frac{c^2k^2}{\omega_{pe}^2} - \frac{c_a^2k^2}{\omega^2} + \frac{i\nu_{ei}}{\omega}\frac{c^2k^2}{\omega_{pe}^2}\right)\underline{E}$$

$$+ \left(\frac{c_a^2}{\omega^2} - \frac{c^2}{\omega_{pe}^2} - \frac{i\nu_{ei}}{\omega}\frac{c^2}{\omega_{pe}^2}\right)(\underline{k}\cdot\underline{E})\underline{k}$$

$$- \frac{c_a^2}{B_o^2\omega^2}\left[(\underline{k}\cdot\underline{E})(\underline{k}\cdot\underline{B}_o) - k^2(\underline{E}\cdot\underline{B}_o)\right]\underline{B}_o$$

$$- \frac{ic}{4\pi n_o e\omega}\left[(\underline{k}\cdot\underline{E})(\underline{k}\times\underline{B}_o) - k^2(\underline{E}\times\underline{B}_o)\right]$$

$$- \frac{c_s^2k^2/\omega^2}{(1 - c_s^2k^2/\omega^2)}\left\{\frac{i(1-g)}{4\pi\, n_o e\omega}\left[\underline{E}\cdot(\underline{k}\times\underline{B}_o)\right]\underline{k}\right.$$

$$\left. + \frac{c_a^2}{B_o^2\omega^2}\left[\underline{E}\cdot(\underline{k}\times\underline{B}_o)\right](\underline{k}\times\underline{B}_o)\right\} = 0$$

where

$$g = \frac{\gamma_i T_i}{\gamma_e T_e + \gamma_i T_i}$$

γ_j being the ratio of specific heats for each component. The above equation differs from that given by Stringer by the inclusion of collision terms in the first two brackets. Scalar multiplying this equation by $\underline{k}$, $\underline{B}_o$ and $\underline{k}\times\underline{B}_o$ in turn will give three equations for $\underline{k}\cdot\underline{E}$, $\underline{E}\cdot\underline{B}_o$ and $\underline{E}\cdot(\underline{k}\times\underline{B}_o)$. Setting the determinant of the coefficients equal to zero gives the dispersion relation,

$$\left[\cos^2\phi - \frac{\omega^2}{k^2c_a^2}\left(Q + \frac{i\nu_{ei}}{\omega}\frac{k^2c^2}{\omega_{pe}^2}\right)\right]\left[\left(\cos^2\phi - \frac{\omega^2}{k^2c_s^2}\right)\right.$$

$$\left. - \frac{\omega^2}{k^2c_a^2}\left(Q + \frac{i\nu_{ei}}{\omega}\frac{c^2k^2}{\omega_{pe}^2}\right)\left(1 - \frac{\omega^2}{k^2c_s^2}\right)\right]$$

$$= \frac{\omega^2}{\omega_{ci}^2}\cos^2\phi\left(1 - \frac{\omega^2}{k^2c_s^2}\right) \qquad \text{(C.9)}$$

This can be compared to Eq. (C.8) to see the modifications due to collisions.

This equation is to be solved specifically for the high frequency Alfvén wave propagating perpendicular to the magnetic field. For $\phi = \pi/2$ the relation is

$$-\frac{\omega^2}{k^2c_a^2}\left(Q + \frac{i\nu_{ei}}{\omega}\frac{k^2c^2}{\omega_{pe}^2}\right)$$

$$\left[-\frac{\omega^2}{k^2c_s^2} - \frac{\omega^2}{k^2c_a^2}\left(Q + \frac{i\nu_{ei}}{\omega}\frac{c^2k^2}{\omega_{pe}^2}\right)\left(1 - \frac{\omega^2}{k^2c_s^2}\right)\right] = 0$$

The last term gives the high frequency Alfvén wave.

$$\frac{1}{c_s^2} + \frac{1}{c_a^2}\left(Q + \frac{i\nu_{ei}}{\omega}\frac{c^2k^2}{\omega_{pe}^2}\right)\left(1 - \frac{\omega^2}{k^2c_s^2}\right) = 0$$

or

$$\omega^3 + \omega^2\, i\nu_{ei}\frac{c^2k^2}{\omega_{pe}^2}\frac{1}{Q} - k^2\frac{(c_a^2 + c_s^2\, Q)\omega}{Q}$$

$$- k^2c_s^2\, i\nu_{ei}\frac{c^2k^2}{\omega_{pe}^2}\frac{1}{Q} = 0 \qquad \text{(C.10)}$$

It can be noticed that without the collision term the undamped high frequency Alfvén wave dispersion relation is recovered.

$$\omega^2 = k^2 \frac{(c_a^2 + c_s^2 Q)}{Q}$$

The imaginary part of ω can be obtained by writing ω in real and imaginary parts

$$\omega = \omega_r - i\omega_i$$

The real equation is from (C.10)

$$\omega_r^3 - 3\omega_i^2 \omega_r - \nu_{ei} \frac{k^2 c^2}{\omega_{pe}^2} \frac{2\omega_i \omega_r}{Q} - \frac{k^2 (c_a^2 + c_s^2 Q) \omega_r}{Q} = 0 \qquad \text{(C.11)}$$

The imaginary equation is

$$3\omega_i \omega_r^2 - \omega_i^3 + \nu_{ei} \frac{c^2 k^2}{\omega_{pe}^2} \frac{\omega_r^2}{Q} - \nu_{ei} \frac{c^2 k^2}{\omega_{pe}^2} \frac{\omega_i^2}{Q}$$

$$- \frac{k^2 (c_a^2 + c_s^2 Q) \omega_i}{Q} - k^2 c_s^2 \nu_{ei} \frac{c^2 k^2}{\omega_{pe}^2} \frac{1}{Q} = 0 \qquad \text{(C.12)}$$

Using the standard assumption

$$\omega_r >> \omega_i \ , \ \nu_{ei}$$

the real and imaginary parts are

$$\omega_r^2 = k^2 \frac{(c_a^2 + c_s^2 Q)}{Q} \qquad \text{(C.13)}$$

and

$$\omega_i = \frac{\nu_{ei}}{2} \frac{k^2c^2}{\omega_{pe}^2} \frac{c_a^2}{(c_a^2/Q + c_s^2)} \frac{1}{Q^2} \tag{C.14}$$

The real frequency is unaffected by light damping. Equation (C.14) agrees with an equation that can be derived from Akhiezer et al.[1] in the limit $Q \approx 1$. This provides a check on the accuracy of the derivation.

The assumption $\omega_r > \nu_{ei}$ is not valid for the dense Z-pinch plasma to be studied in Chapter V. Thus, the dispersion relation will have to be derived without using that assumption. Equations (C.11) and (C.12) are exact. ω_r can be eliminated from (C.12) by using (C.11). This gives

$$\omega_i^3 + \nu_{ei} \frac{k^2c^2}{\omega_{pe}^2} \frac{\omega_i^2}{Q} + \left[k^2 \frac{(c_a^2/Q + c_s^2)}{4} + \frac{\nu_{ei}^2}{4} \left(\frac{k^2c^2}{\omega_{pe}^2} \right)^2 \frac{1}{Q^2} \right] \omega_i + \frac{\nu_{ei}}{8} \frac{k^2c^2}{\omega_{pe}^2} \frac{1}{Q} k^2 c_a^2 = 0 \tag{C.15}$$

which contains ω_i alone. The equation for ω_r is then

$$\omega_r = \left[3\omega_i^2 + \nu_{ei} \frac{k^2c^2}{\omega_{pe}^2} \frac{2\omega_i}{Q} + k^2 \left(\frac{c_a^2}{Q} + c_s^2 \right) \right]^{1/2} \tag{C.16}$$

Equation (C.15) for ω_i is a cubic equation. When values for the parameters ν_{ei}, ω_{pe}, etc., are substituted, this equation can easily be solved by computer. One real root and a complex pair of roots are expected. Since ω_i is assumed real, the real root is correct. Once ω_i is known, its value may be substituted into Eq. (C.16) to obtain ω_r. Calculations performed for Chapter V show

$$\omega_r >> \omega_i$$

so the correction to the real frequency due to damping is negligible.

REFERENCES

1. Akhiezer, A.I., I.A. Akhiezer, P.V. Polovin, A.G. Sitenko, and K.N. Stepanov, Plasma Electrodynamics (Pergamon Press, New York, 1975), Vol. 1, p. 59.

2. Briggs, R.J., Electron-Stream Interactions (MIT Press, Cambridge, 1964), p. 39.

3. Brueckner, K.A. and S. Jorna, Rev. Mod. Phys. 46, 325 (1974).

4. Chapin, D., J.J. Duderstadt, and D.R. Bach, J. Applied Phys. 45, 1726 (1974).

5. Clemmow, P.C. and J.D. Dougherty, Electrodynamics of Particles and Plasmas (Addison-Wesley Publishing Co., Reading, 1969), p. 290.

6. DeBoo, J.C. and D.R. Bach, J. Applied Phys. 46, 2496 (1975).

7. Drake, J.F. et al., Phys. Fluids 17, 778 (1974).

8. Duderstadt, J.J., R.S.B. Ong, D.P. Duston, and D.J. Kenney, University of Michigan, Technical Report #013746-2-T, 1976 (unpublished).

9. Formisano, V. and C.F. Kennel, J. Plasma Phys. 3, 55 (1969).

10. Forslund, D.W., J.M. Kindel, and E.L. Lindman, Phys. Fluids 18, 1002 (1975).

11. Gorbunov, L.M., JETP 28, 1220 (1969).

12. Kaw, P.K., in Advances in Plasma Physics, edited by A. Simon (Wiley-Interscience Publishers, New York, 1975), Vol. 6, p. 207.

13. Kaw, P.K. and J. Dawson, Phys. Fluids 12, 2586 (1969).

14. Krall, N.A. and A.W. Trivelpiece, Principles of Plasma Physics (McGraw-Hill Book Company, New York, 1973), p. 390.

15. Landau, L.D. and E.M. Lifshitz, Electrodynamics of a Continuous Medium (Addison-Wesley Publishing Co., Reading, 1960), p. 64.

16. Lee, K.F., Phys. Fluids 17, 1343 (1974).

17. Liu, C.S., in Advances in Plasma Physics, edited by A. Simon (Wiley-Interscience Publishers, New York, 1975), Vol. 6, p. 121.

18. Manheimer, W.M. and E. Ott, Phys. Fluids 17, 1413 (1974).

19. Massey, R., K. Berggren, and Z.A. Pietrzyk, PRL 36, 963 (1976).

20. Nishikawa, K., J. Phys. Soc. of Japan 24, 916 (1968).

21. Nishikawa, K. and C.S. Liu, in Advances in Plasma Physics, edited by A. Simon (Wiley-Interscience Publishers, New York, 1975), Vol. 6, p. 3.

22. Nucholls, J., L. Wood, A. Thiessen, and G. Zimmerman, Nature 239, 139 (1972).

23. Offenburger, A.A., M.R. Cervenan, A.M. Yam, and A.W. Pasternak, J. Applied Phys. 47, 1451 (1976).

24. Pesme, D., G. Laval, and P. Pellat, PRL 31, 203 (1973).

25. Rosenbluth, M.N., PRL 29, 565 (1972).

26. Schmidt, G., Physics of High Temperature Plasmas (Academic Press, New York, 1966), p. 47.

27. Shukla, P.K., M.Y. Yu, and K.H. Spatschek, Phys. Fluids 18, 265 (1975).

28. Spitzer, L., Physics of Ionized Gases (Wiley-Interscience Publishers, New York), p. 23.

29. Stamper, J.A. et al., PRL 26, 1012 (1971).

30. Stamper, J.A. and D.A. Tidman, Phys. Fluids 16, 2024 (1973).

31. Stamper, J.A. et al., in Laser Interactions and Related Plasma Phenomena, edited by H. Hora and H. Schwarz, (Plenum Press, New York, 1974), Vol. 3B, p. 713.

32. Stamper, J.A. and B.H. Ripin, PRL 34, 138 (1975).

33. Steel, D.G., P.D. Rockett, P.L. Colestock, and D.R. Bach, Bull. APS 20, 1297 (1975).

34. Steel, D.G., Ph.D. thesis, University of Michigan (1976).

35. Stringer, T.E., Plasma Physics 5, 89 (1973).

36. Tanenbaum, S.B., Plasma Physics (McGraw-Hill Book Co., New York, 1967), p. 82.

37. Tidman, D.A. and R.A. Shanney, Phys. Fluids 17, 1207 (1974).

38. Thomson, J.J., C.E. Max, and K. Estabrook, PRL 35, 663 (1975).

39. Turechek, J.J. and F.F. Chen, PRL 36, 720 (1976).

40. Winsor, N.K. and D.A. Tidman, PRL 31, 1044 (1973).

41. Yu, M.Y., K.H. Spatschek, and P.K. Shukla, Z. Naturforsch 29a, 1736 (1974).